The isolation, characterisation, gas phase electron diffraction and crystal structure of the thermally stable radical [CF₃CSNSCCF₃]· †

Scott Brownridge,[a] Hongbin Du,[a] Shirley A. Fairhurst,[b] Robert C. Haddon,[c]
Heinz Oberhammer,[d] Simon Parsons,[e] Jack Passmore,*[a] Melbourne J. Schriver,[f]
Leslie H. Sutcliffe[g] and Nicholas P. C. Westwood[h]

[a] *Department of Chemistry, University of New Brunswick, Post Office Box 45222, Fredericton, New Brunswick, E3B 6E2, Canada. E-mail: passmore@unb.ca*
[b] *Nitrogen Fixation Laboratory, John Innes Centre, Norwich, UK NR4 7UA*
[c] *Department of Chemistry and Physics, and Advanced Carbon Materials Center, University of Kentucky, Lexington, Kentucky, 40506, USA*
[d] *Institut fur Physikalische und Theoretische Chemie, Universitat Tuebingen, 72076 Tuebingen 1, Auf der Morganstralle 8, Germany*
[e] *Department of Chemistry, University of Edinburgh, Edinburgh, UK EH9 3JJ*
[f] *Department of Science, Atlantic Baptist University, P.O. Box 6004, Moncton, New Brunswick, E1C 9L7, Canada*
[g] *Chemistry and Physics Departments, University of Surrey, Guildford, Surrey, UK TW16 7LN*
[h] *Department of Chemistry and Biochemistry, University of Guelph, Guelph, Ontario, N1G 2W1, Canada*

The first structural characterisation of a heterocyclic free radical in all phases has been achieved. 4,5-Bis(trifluoromethyl)-1,3,2-dithiazol-2-yl, [CF₃CSNSCCF₃]· **4d**, a 7π radical, was prepared quantitatively on reduction of **[4d][AsF₆]** with various reducing agents. It is a blue gas over a green paramagnetic liquid [¹⁹F NMR δ −59.7], which freezes to a diamagnetic black-green solid. There is a remarkably large volume increase on melting implying that the liquid consists of discrete monomeric radicals, and consistently there is no tendency to dimerise in CCl₃F solution and the vibrational spectra attributable to the monomer are essentially identical in all phases. The thermodynamic properties obtained for the vapourisation, sublimation and melting processes are very similar to those of related diamagnetic materials. **4d** is remarkably thermochemically robust giving decomposition products identical to those from photochemical decomposition, a quantitative mixture of CF₃CSSCCF₃ (and its oligomers) and CF₃CNSNCCF₃. The reaction chemistry is described. The crystal structure shows radical **4d** to be a planar heterocyclic ring which associates in the solid as a diamagnetic tetramer. The structure of the gaseous monomer determined by electron diffraction is very similar to that in the solid phase. Comprehensive physical measurements were made including the UV-visible spectra of the bright blue solutions, variable temperature magnetic susceptibility and quantitative variable temperature ESR spectra both of which confirm a phase change from a diamagnetic solid to a paramagnetic liquid on melting, the vibrational spectra, and the photoelectron spectrum of the gaseous free radical. A study of the behavior of RCSNSCR· (R = H, CH₃ or CF₃) given by the reduction of RCSNSCR⁺ on increase of concentrations of radical is reported, including the isolation of HCSNSCCF₃· at low temperature. The experimental and calculated [UMPW1PW91/6-31+G*] structures of **4d** are in good agreement. These and related calculations also support the interpretation of the vibrational and photoelectron spectra, and the thermodynamic properties of **4d**, as well as provide possible explanations for the relative stabilities of RCSNSCR·, and imply that the weak intramolecular interactions in **4d** in the solid state are largely ionic S^{δ+}···N^{δ−} interactions.

Introduction

The preparation of new ionic or neutral heterocycles that incorporate π bonds to the heavier elements of Groups 15 and 16 has been the subject of much interest in recent years.[1] Motivation has included the stabilisation of new π environments for these elements and the search for compounds, especially radicals, having novel and/or desirable physical, chemical, or biological properties.[2] Of particular note is the recent synthesis by Oakley, Haddon and co-workers of a C/N/S neutral heterocycle that is a π molecular conductor[3] and by Banister, Rawson and co-workers of the beta phase of [p-NCC₆F₄CNSSN]·, a spin canted weak ferromagnetic material below 36 K.[4] Our interest in this area arose from our discovery of the quantitative, symmetry allowed cycloaddition of [SNS]⁺ ([SNS]-[AsF₆]) to a wide range of unsaturated centres[5,6] as shown in Schemes 1 and 2 in reference 7, providing general routes to [SNS]⁺ containing heterocycles, several of which were previ-

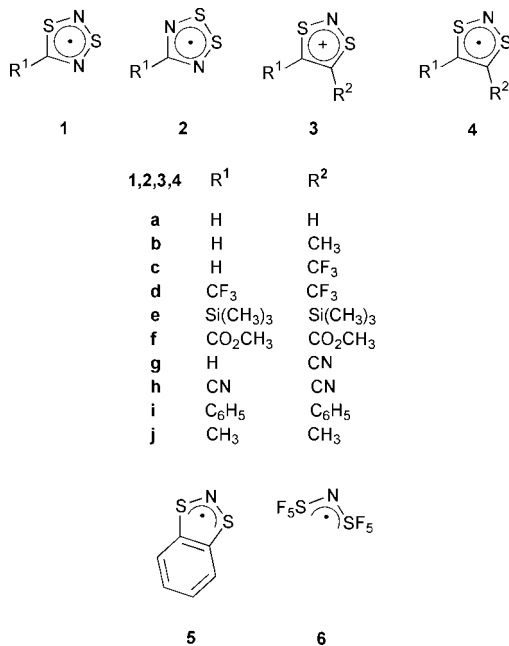DOI: 10.1039/b001489n

J. Chem. Soc., Dalton Trans., 2000, 3365–3382 **3365**

ously unknown. Radicals **1**, **2** and **4** are members of a larger family of sulfur–nitrogen containing heterocyclic radicals, the archetype of which is the 7π [$\overline{SNSNS}$]$^+$ cation first structurally elucidated by Banister *et al.* in 1974.[8] Isovalent substitution into the ring of this radical generates families of related ring systems demonstrated in Scheme 1. Remarkably, most of these hetero-
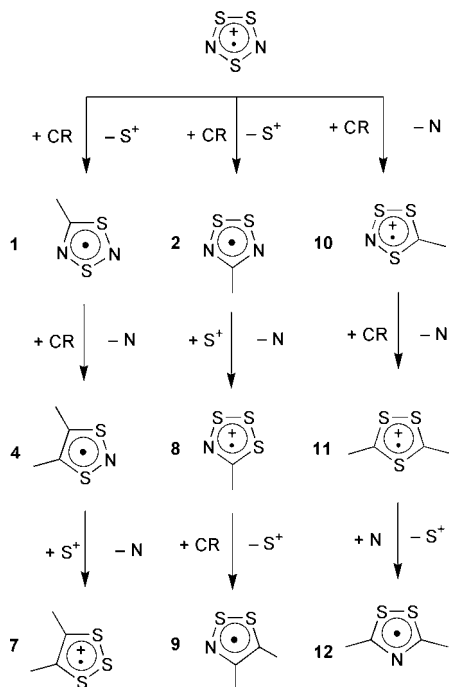
Scheme 1

cycles are known and have been shown to have rich synthetic and structural chemistries. We recently reported the first derivatives of ring systems **7**[9] and **8**.[10]

1,2,3,4	R^1	R^2
a	H	H
b	H	CH_3
c	H	CF_3
d	CF_3	CF_3
e	$Si(CH_3)_3$	$Si(CH_3)_3$
f	CO_2CH_3	CO_2CH_3
g	H	CN
h	CN	CN
i	C_6H_5	C_6H_5
j	CH_3	CH_3

Reduction of [RĊSNSN]$^+$ led to the quantitative synthesis of the corresponding radical **1**, which in some cases was isolatable [R = ^{t}Bu, C_6H_5 or p-$C_6H_4NO_2$[11]]. However these derivatives, and those radicals which were not isolatable, undergo a photochemically and/or thermally symmetry allowed rearrangement[12] *via* a dimer intermediate to the thermodynamically more stable isomer **2**, first prepared by Banister and co-workers.[13] The net result is a switching of positions of adjacent

cyclic sulfurs and nitrogens, which is unprecedented in main group chemistry. The reduction of **3** [RĊSNSĊR]$^+$ gives the corresponding [RĊSNSĊR]$^{\bullet}$ **4** quantitatively in dilute solution, readily detectable by ESR.[14] Some radicals of this family had been prepared previously by Sutcliffe and co-workers from the reaction of S_4N_2 with alkynes in dilute solution and detected by ESR spectroscopy.[15] The authors noted that derivative [CF_3ĊSNSĊCF$_3$]$^{\bullet}$ **4d** showed considerable persistence as a free radical but no attempt to isolate and characterise the radical as a pure material was reported. This implied stability is consistent with a number of persistent radicals containing a central SNS moiety attached to electronegative groups that are reported to be stable in dilute solution, such as the dithiazolyl radical [CF_3ṠNSCF$_3$]$^{\bullet}$.[16,17] The acyclic radical, [F_5ṠNSF$_5$]$^{\bullet}$ **6** has also been shown to be stable enough to allow identification and characterisation by ESR in dilute solution. The dissociation of this radical to stable diamagnetic species has made the complete characterization of this compound difficult.[18]

Very few of the simple derivatives of the radical **4** have actually been isolated and characterised. Wolmershäuser *et al.* were the first to isolate and characterise a 1,3,2-dithiazolyl radical **5** (discovered by Sutcliffe and co-workers[15]), fused to an aromatic ring, as a pure compound.[19] Subsequent investigation has shown that **5** is monomeric in dilute solution with the stable diamagnetic dimer actually isolated.[20] This spawned a substantial body of research on 1,3,2-dithiazolyl radicals fused to aromatic systems including recent research on systems with multiple radical centres.[21] In 1987 we reported, in a preliminary communication,[22a] on the isolation and initial characterisation of a derivative of **4**, the thermally stable **4d**, for the first time. More recently, the 4,5-dicyano-1,3,2-dithiazolyl radical **4h**[23] has been isolated by Wolmershäuser and Kraft and shown to have a similar stability to those of **5** and **4d**.

Our preparative route to simple derivatives of radical **3**, and hence **4,** from alkynes is very general and in this paper we describe the preparation and relative stabilities of a range of derivatives of **4** in solution. Possible explanations for the relative stabilities of **4** are implied by theoretical calculations. We were able to isolate **4c** in small quantities at low temperature. However, of the derivatives of **4** we attempted to prepare, only **4d** was isolable under ambient conditions. It is a green volatile liquid under a blue gas at room temperature and herein we give an account of the characterisation of its structure, spectroscopic and physical properties, including a proposed structure of the liquid inferred from its physical properties, and the relationship between structures in all phases. The structural and spectroscopic interpretations are assisted by theoretical calculations. **4d** is of particular interest as it is a liquid and paramagnetic under ambient conditions, and when initially isolated[22a] was the first example of a class of materials we called the *Paramagnetic liquids* ‡.[22b] Other examples that are liquids under ambient conditions include ^{t}BuĊNSNS and the isomeric ^{t}BuĊNSSN.[22b] In addition, some related solids that are diamagnetic solids at room temperature become paramagnetic liquids on melting. We also report a preliminary investigation of the chemistry of **4d**.

Experimental

Reagents and general procedures

Apparatus, techniques and chemicals unless specified have been

---

‡ We define a paramagnetic phase as the lowest energy phase in which the compound exhibits bulk paramagnetism consistent with a near stoichiometric number of unpaired electrons. Thus a *paramagnetic gas* is paramagnetic only in the gas phase, a *paramagnetic liquid* is paramagnetic in the gas and liquid phases and diamagnetic in the solid. A *paramagnetic solid* is paramagnetic in all phases.

Table 1 Preparations of radical **4d**

Reactant (g, mmol)	Reducing agent or other compound (g, mmol)	SO_2 (g)	Apparent reaction time[a]	4d g	mmol	%[b]	Non-volatile residue
3d[AsF₆]							
5.864, 13.67	$Na_2S_2O_4$[c] (7.09, 40.80)	8.49	24 h	2.68	11.15	82	Insoluble white solid ($Na_2S_2O_4$, AsF_6^-; IR)
0.429, 1.00	$(C_6H_5)_3Sb$ (0.175, 0.50) $N(CH_3)_4Cl$ (0.110, 1.00)	5.10	< 5 min	0.19	0.80	80	Insoluble white solid ($N(CH_3)_4AsF_6$; IR) Soluble yellow solid ($N(CH_3)_4Cl$, $N(CH_3)_4AsF_6$, $(C_6H_5)_3Sb$ and $(C_6H_5)_3SbCl_2$; IR)
0.877, 2.04	KI (0.344, 2.07)	7.08	< 5 min	0.393	1.64	80	Insoluble white solid ($KAsF_6$, IR; 0.356 g) Insoluble sublimed black solid (I_2, mp)
3d[Cl]							
0.086, 0.31	$(C_6H_5)_3Sb$ (0.063, 0.18)	3.55	< 5 min[d]	0.072	0.20	97	Non-volatile yellow-white solid ($(C_6H_5)_3SbCl_2$, $(C_6H_5)_3Sb$ (IR, 0.07 g)

[a] Assumed to be from the initial warming to r.t. until formation of an opaque black solution. [b] The reaction yield (of the isolated triply distilled product) based on **3d[AsF₆]**. [c] The reactants (**3d[AsF₆]** and $Na_2S_2O_4$) were intimately ground to a fine powder prior to the reaction. No apparent reaction occurred between the solids. [d] An initial reaction was observed between the two solids prior to the addition of the solvent giving a blue vapour over the darkened solids.

described.[24] Chemical analyses were by Beller Micro-analytisches Laboratorium. Reactions were generally carried out in two bulb Pyrex vessels incorporating two J. Young Teflon-in-glass valves and a medium sintered glass frit separating the two bulbs (approximately 20 mL volume each).[25] The radical **4d** is photosensitive; therefore it was prepared and handled with a minimum exposure to light.

$Na_2S_2O_4$, $(C_6H_5)_3Sb$ and $[(CH_3)_4N][Cl]$ [Aldrich] were used as received. **3d[AsF₆]**, $[CF_3\overline{CSNSCH}][AsF_6]$, $[H\overline{CSNSCH}][AsF_6]$ and $[H\overline{CSNSCCH_3}][AsF_6]$ were prepared according to reference 5(*a*), $[CH_3CO_2\overline{CSNSCCO_2CH_3}][AsF_6]$ and $[(CH_3)_3SiCSNSCSi(CH_3)_3][AsF_6]$ according to reference 5(*b*). Infrared spectra were recorded on a Perkin-Elmer Model 683 spectrometer, ^{1}H and ^{19}F NMR spectra as previously reported[5] and FT-Raman spectra from neat samples sealed under nitrogen in thick walled precision 5 mm NMR tubes (Wilmad Glass, Buena, NJ) on an FT-IR spectrometer (Bruker IFS66) equipped with a FT-Raman accessory (Bruker FRA 106), as previously described.[24]

UV-visible spectra were recorded on a Perkin-Elmer Model 330 UV-visible spectrometer in the range 185–1000 nm. The He(I) photoelectron spectrum of radical **4d** was obtained from the vapor above the liquid at the University of Guelph on an instrument specifically designed to study labile species and calibrated with Ar and CH_3I.[26] Resolution was 45 meV during data acquisition.

Solution ESR spectra were recorded using a locally modified version of a Varian E-4 spectrometer fitted with an external temperature control unit (University of New Brunswick). X-Band spectra were recorded at the Royal Holloway College with a Varian E-4 spectrometer: details of sample manipulation, spectrometer calibration and *g*-factor measurements have been given previously.[15] Curie and *Q*-factor corrections were made for intensity measurements: the latter correction was made after examining $CFCl_3$ with an external sample of polycrystalline DPPH (diphenylpicrylhydrazyl). Liquid state X-band spectra were obtained with a Varian E9 ESR spectrometer fitted with a dual cavity, which enabled *Q*-factor corrections to be made with a polycrystalline DPPH sample in the second cavity.

Mass spectra were recorded on a VG 70780 E mass spectrometer with an ionising voltage of 70 eV (University of Durham, Durham, England).

Magnetic susceptibilities were determined by the Gouy method (University of New Brunswick) using a Newport 1–1/2 inch electromagnet in conjunction with a Stanton Instruments Model MC5 microbalance with a sensitivity of ±0.02 mg or by the Faraday method (AT & T Bell Laboratories) using an apparatus that has been described previously.[21]

Melting points were uncorrected.

The preparation of radical 4d

In a typical reaction a sample of **3d[AsF₆]** and an excess of reducing agent were loaded into one bulb of a two-bulb vessel. Sulfur dioxide was then condensed onto the mixture and the vessel wrapped in aluminium foil. The mixture was stirred at room temperature for twenty-four hours, changing from an initial clear yellow to opaque black. It was filtered and the insoluble material washed several times with the solvent by back condensation. The volatile materials were removed to a U-tube trap ($-196\,°C$) *via* a dynamic vacuum, and fractionally distilled under a static vacuum by passage through a series of U-tube traps held at -15, -78 and $-196\,°C$, the last two containing SO_2 and trace amounts of **4d** (IR). The $-15\,°C$ U-tube trap contained a black crystalline solid which melted to give a black liquid at r.t. and was fractionally distilled again twice, giving a photosensitive black liquid under a bright blue vapour in the final $-15\,°C$ U-tube trap. This black liquid was shown to be pure radical **4d**, typically by mp, infrared and NMR spectroscopy, and then stored at r.t. in a common reservoir in the dark. Experimental details are given in Table 1. **4d**: mp 11.9–12.5 °C (Found: C, 20.31; F, 46.80; N, 5.87; S, 26.84%; M⁺ *m/z* 240. $C_4F_6NS_2$ requires C, 20.00; F, 47.46; N, 5.83; S, 26.70%; M⁺ *m/z* 240). Infrared and Raman spectra of **4d** are given in Figs. 1 and 2, respectively, with vibrational frequencies and assignments given in Table 2. Mass spectrum [direct inlet, 25 °C, 70 eV]: *m/z* (relative intensity % of highest peak, assignment) 242 (7, $[CF_3\overline{C^{34}SNSCCF_3}]^+$), 241 (5, $[^{13}CF_3\overline{CSNSCCF_3}]^+$), 240 (74, $[CF_3\overline{CSNSCCF_3}]^+$), 221 (4, $[CF_3\overline{CSNSCCF_2}]^+$), 125 (10, $[CF_3C_2S]^+$), 113 (9, $[CF_3CS]^+$), 93 (5, $[CF_3C_2]^+$), 87 (8, unassigned), 80 (10, $[^{34}SNS]^+$), 78 (100, $[SNS]^+$), 76 (5, $[SCS]^+$), 69 (22, $[CF_3]^+$), 64 (6, S_2^+), 46 (32, $[SN]^+$), 40 (11, $[CN_2]^+$) and 32 (93, S⁺). UV-visible spectrum: Solution [quartz cell, path length = 1 mm] (hexane, 0.0453 M), λ 560 (ε 260), 738 (110); (hexane, 0.0063 M) 227 (2260), 287 (2720) [Fig. 3]; Gas phase [quartz cell, path length = 10 cm, gas, r.t.] 282 (1450), 544 (40) and 708 nm (80 M⁻¹ cm⁻¹). Acquisition of more than one spectrum from a single sample led to the appearance of bands in the region of 330 and 418 nm that were also observed in the spectra of the photolytic decomposition products. ^{19}F NMR spectrum: in SO_2 solution [0.0077 g, 0.032 mmol **4d**, 0.022 g, 0.17 mmol CCl_3F, 0.93 g SO_2 in a thick walled 5 mm o.d. NMR tube at r.t.] δ (assignment, integration)
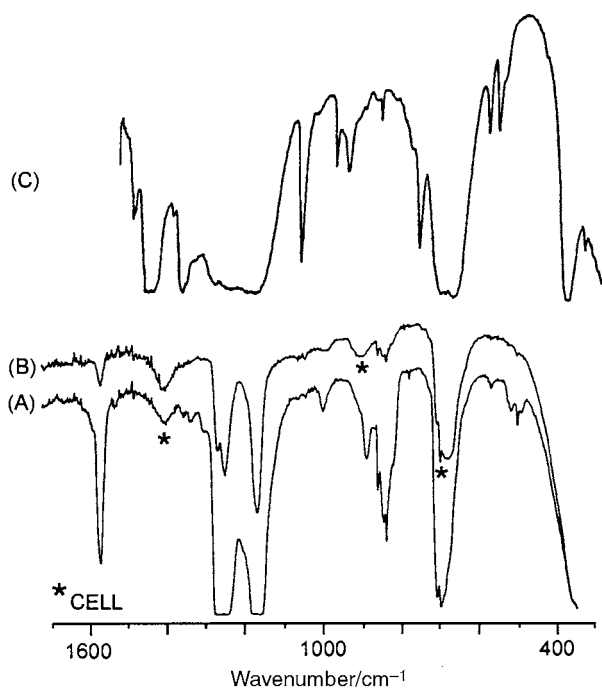
Fig. 1 The infrared spectra of radical **4d** at (A) $P = 20$ mmHg, (B) $P = 1$ mmHg, and of **3d[AsF$_6$]** (C).
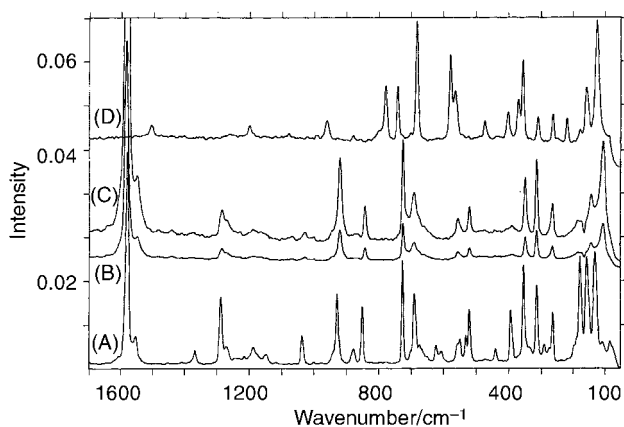

Fig. 2 FT-Raman spectra of radical **4d** as a frozen solid at 150 K (A), neat liquid at r.t. (B), close-up of the neat liquid at r.t. (C) and of **3d[AsF$_6$]** at 150 K (D).

0 (CCl$_3$F, 0.97), -53.7 (< 0.01, a hydrolysis product, unknown), -55.7 (< 1, unknown), -56.5 (< 1, unknown), -62.6 (< 0.01, CF$_3$$\overline{\text{CSSC}}CF_3$) and -66.6 [< 1, a hydrolysis product, unknown] (the total integration for the non-CCl$_3$F resonances = 0.03); in spectra obtained from other samples additional resonances were observed at δ -42.3, -61.9 (CF$_3$$\overline{\text{CNSNC}}CF_3$) and -76.0; Neat liquid (0.440 g, 5 mm o.d. thick walled NMR tube), δ -59.7, $\nu_{1/2} = 200$ Hz, integration = 0.98 and three smaller resonances (δ -42, -55, -62, total integration = 0.02). Estimated concentration of fluorine in sample by comparison of standard solutions of CCl$_3$F in SO$_2$, 32 M (based on the density of CF$_3$$\overline{\text{CSNSC}}CF_3$, 40.5 M). Conductivity: a Pyrex vessel consisting of a 20 mm o.d. tube with a flat bottom and a J. Young valve was fitted with platinum wire electrodes that ended in flattened blades of approximately 0.8 cm² area, 0.5 cm apart. The blades of the electrodes were immersed in radical **4d**. In both the liquid and solid state **4d** was non-conductive. Density: liquid (22 °C), 1.63 ± 0.02 g cm^{-3}, solid (-78 °C), $\rho \geq 1.97 \pm 0.02$ g cm^{-3} ($\rho = 2.086$ g cm^{-3}; calculated from crystallographic data at -90 °C).
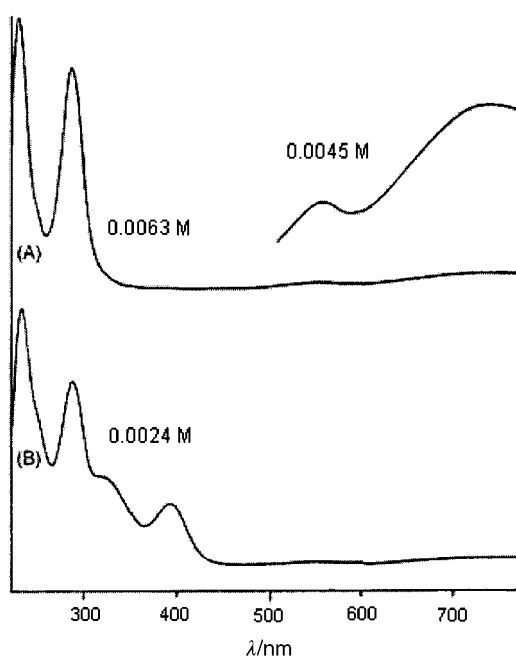
Fig. 3 The UV-visible spectrum of radical **4d**, (A) in hexane after 1 h, (B) After 19 h, with 9 h of irradiation at 544 nm in the spectrometer.

Vapour pressure (VP). At 22 °C, vapour over neat liquid, vapour pressure 25 mmHg, measured by Penning gauge. A sample of pure radical **4d** was contained in one arm of a sealed mercury manometer immersed in a large (20 L), stirred, water bath heated with immersion heaters in a slightly modified procedure to that given in reference 28, in a darkened room. For the solid a shorter manometer was used with only the sample bulb cooled in a low temperature bath. The measurements were repeated on the same samples without significant changes in the data, indicating that decomposition had not occurred during the experiment. A full description is given in ref. 25. The plots of ln VP *versus* 1000/T gave straight lines by least squares analysis (correlation coefficients of 0.993 (liquid) and 0.999 (solid) defined by eqns. (1) and (2). Experimental data are included with the Supplementary Materials.

$$\ln \text{VP}_{[4d] (l)} = (-4580/T) + 18.3 \qquad (1)$$

$$\ln \text{VP}_{[4d] (s)} = (-5844/T) + 22.5 \qquad (2)$$

ESR spectrum. At 10^{-3} M in CCl$_3$F, -70 °C: $g = 2.0052$, $a^{\text{N14}} = 1.125$ mT, $a^{\text{F19}} = 0.069$ mT. Pattern is a $1:1:1$ triplet of $1:6:20:25:20:6:1$ septets as reported in reference 15. Neat liquid: radical **4d** was sealed in a capillary (2 mm o.d.). The sample was quench frozen in liquid nitrogen and kept immersed for approximately six hours and then placed in one section of the ESR dual cavity and warmed in stages from 121 K. The relative concentrations of unpaired electrons in the cavity were obtained after making Q and Curie corrections (T(K)/relative concentration (M)): 335/11000, 315/11000, 296/11000, 278/5400, 269/1300, 259/1600, 241/700, 211/400, 181/400 and 151/400, as shown in Fig. 4. 4.35 M in CCl$_3$F: the sample was examined above the freezing point of the solution and the relative concentration of unpaired electrons did not significantly change, T(K)/relative concentration (M) 318/4.35, 298/4.35, 283/4.35, 267/4.27 and 226/4.18.

Magnetic susceptibility. Gouy method (calibrated with solid Hg[Co(CNS)$_4$]). The diamagnetic correction for radical **4d** was 84.42 × 10^{-6} cgs mol^{-1}. Solid (0 °C); $\chi_m^* = -5$ (± 45) × 10^{-6} cgs mol^{-1}, $\mu_{\text{eff}} = -0.02$ (± 0.33) μ_B. Neat Liquid (23 °C); $\chi_m^* = 969$ (± 23) × 10^{-6} cgs mol^{-1}, $\mu_{\text{eff}} = 1.50$ (± 0.02) μ_B. Solution: (CCl$_3$F, 1.16 M, 23 °C) $\chi_m^* = 1476 × 10^{-6}$ cgs, $\mu_{\text{eff}} = 1.86$ μ_B;

Table 2 Comparison of vibrational data for radical **4d** and **3d** in **3d[AsF₆]**

3d[AsF₆]				4d				
IR [a]	FT-Raman [b]	Calculated [c]	Assignment [d]	Gas phase IR	FT-Raman r.t. liquid, neat [b]	FT-Raman frozen, neat [b]	Calculated [c]	Assignment [d]
		36 (vw, 0.7)	CF₃ twist				20 (vw, 0.4)	CF₃ twist
		38 (vw, 1)	CF₃ twist				47 (vw, 0.2)	CF₃ twist
		94 (vw, 15)	δCSN sym. out of plane				91 (vw, 5.4)	δCSN out of plane
	115 (100)	101 (0.4, 1)	δCCC + δSCC		105 (14)	109 (7)	110 (0.1, 0.1)	δCCC + δSCC
					142 (7)	131 (69)	127 (0.6, 3)	δCCC + δSNS
	159 (47)	135 (0.4, 9)	δSCC + δSNS out of plane			157 (54)	155 (0.5, 0.1)	δSNS + δCSN out of plane
	178 (9)	162 (0.2, 1)	ring + CF₃ rock		186 (2)	178 (56)	176 (0.2, 0.1)	ring + CF₃ rock
	220 (9)	249 (0.6, 11)	ring + CF₃				253 (vw, 0.5)	ring + CF₃
	264 (13)	254 (vw, 0.5)	ring + CF₃		265 (4)	265 (16)	253 (0.5, 4)	ring + CF₃
	311 (11)	293 (0.4, 14)	ring + CF₃ breathe			291 (8)	301 (0.3, 4)	ring + CF₃
	357 (36)	336 (1, 28)	ring + CF₃ breathe, ν₅[AsF₆]⁻		315 (7)	315 (28)	335 (0.3, 7)	ring + CF₃
	371 (24)	383 (1, 14)	δSNS/ring		350 (5)	356 (52)	372 (vw, 0.7)	ring
	402 (18)	387 (2, 6)	δSNS out of plane		390 (1)	395 (24)	417 (0.2, 0.2)	δSCC sym. out of plane
		444 (0.3, 2)	δ_sym CSN out of plane + δ_sym SCC		446 (1)	441 (6)	484 (vw, 1)	δSCC out of plane/CF₃
	474 (12)	490 (vw, 3)	δSCC out of plane/CF₃		475 (1)	472 (1)	505 (0.7, 1)	δSNS/δCSN
		533 (0.1, 3)	δCF₃/νCS asym.		521 (2)	522 (18)	522 (0.9, 0.8)	δCF₃/νCS asym.
		534 (0.1, 6)	δCF₃/νCS sym., ν₂]AsF₆]⁻			532 (8)	532 (0.1, 3)	δCF₃
	564 (25)	566 (2, 69)	δCSN + δSNS	543w	557 (3)	550 (14)	571 (0.7, 0.4)	δ_sym(SCC) out of plane
583w	579 (51)	582 (2, 0.2)	δSCC sym. out of plane	590w		607 (5)		
608w						623 (8)	641 (0.1, 12)	δ_sym(SCC) out of plane + νSNS sym.
645m		664 (0.1, 7)	δSCC asym. out of plane		676sh	675sh	660 (1, 6)	νSNS sym. + δ_asym(SCC) out of plane
	683 (79), 700sh	683 (4, 0.8)	ν₁AsF₆⁻/δCF₃/νCS asym.		690 (5)	691 (34)	673 (3, vw)	νCS sym. + δCF₃
694vs	742 (38)	710 (2, 42)	νCS sym. + δCF₃	721s	726 (9)	727 (42)	697 (4, 11)	δCF₃/νCS asym.
779m	779 (46), 800sh	773 (10, 100)	νSNS sym.	843m	843 (2)	852 (24)	830 (1, 3)	νCS sym. + δCF₃
	880 (3)	857 (0.1, 9)	νCS asym./νSNS asym.	863m	872 (1)	878 (6)	853 (1, 0.1)	νSNS asym./νCS asym.
963w	961 (18)	933 (1, 31)	νCS sym.	917m	921 (9)	929 (29)	906 (4, 7)	νSNS asym.
993m	993 (2)	980 (0.2, 5)	νSNS asym.		1000 (1)	1001 (1)		
	1080 (2)	1053 (13, 3)	νCS asym./CF₃	1028m	1027 (2)	1038 (14)	1006 (0.5, 2)	νCS sym.
		1160 (32, 27)	νCF₃			1149 (4)	1142 (0.9, 2)	νCS asym./CF₃
1195s, br		1188 (100, 0.3)	νCF₃	1182vs	1189 (4, br)	1187 (7, br)	1155 (59, 0.5)	νCF₃
	1202 (7)	1205 (15, 11)	νCF₃				1167 (0.1, 2)	νCF₃
		1233 (36, 9)	νCC asym./νCF₃			1216 (3)	1174 (88, 7)	νCF₃
to		1242 (78, 17)	νCC sym./νCF₃	1263vs		1246 (2)	1238 (100, 9)	νCC sym./νCF₃
	1263 (2)	1259 (66, 21)	νCC asym./νCF₃		1269 (2, sh)	1271 (6, sh)		
1299s, br				1282vs	1286 (6)	1288 (27)	1256 (52, 25)	νCC asym./νCF₃
				1316w				
1348w				1350w				
1371w					1373 (1)	1368 (7)		
					1548 (6)	1554 (9)		¹³C isotope effect
1504m	1505 (8)	1497 (2, 88)	ν(C=C)	1580m	1585 (100)	1580 (100)	1596 (12, 100)	ν(C=C)

[a] Nujol mull. [b] Relative intensities in parentheses. [c] UMPW1PW91/6-31+G*, IR and Raman relative intensities in parentheses. vw indicates calculated relative intensities less than 0.1. [d] Based on visualision of calculated vibrations using HyperChem.[27] A plus sign indicates two vibrations of equal intensity; a solidus indicates the first listed vibration is more pronounced than the second.
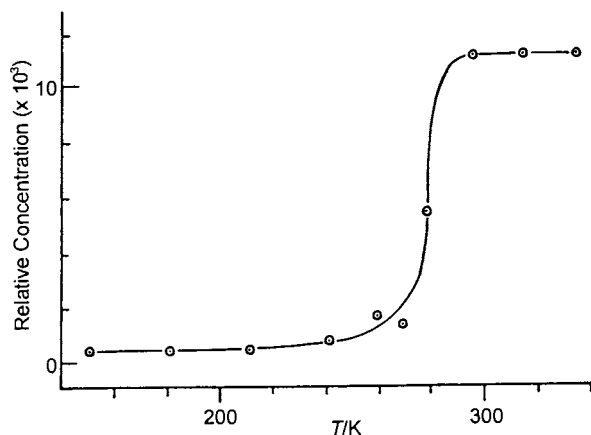
J. Chem. Soc., Dalton Trans., 2000, 3365–3382

3369

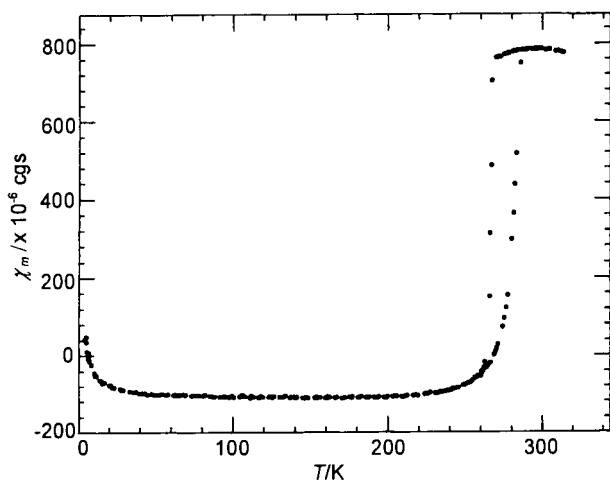**Fig. 4** The relative intensity of the ESR of radical **4d** as a function of temperature.

Fig. 5 The variable temperature magnetic susceptibility of radical **4d**.

(CCl$_3$F, 2.00 M, 23 °C) $\chi_m^* = 1587 \times 10^{-6}$ cgs, $\mu_{eff} = 1.92$ μ_B; (CCl$_3$F, 3.26 M, 23 °C) $\chi_m^* = 1164 \times 10^{-6}$ cgs, $\mu_{eff} = 1.65$ μ_B. A plot of mole fraction of **4d** *versus* the effective magnetic moment gave an extrapolated value of 1.93 μ_B at infinite dilution. Faraday method: the magnetic susceptibility was measured from 4.2 to 380 K. Low temperature data were obtained at intervals of about 1 K by using a helium cryostat cooled at an average rate of 1 K min^{-1}. The absolute accuracy of the susceptibility is ± 2% as determined by a comparison with several standards. The relative accuracy of these measurements is much higher, approximately ± 0.06%, so that small changes can easily be detected. The applied field was 14 kOe, and the measured susceptibility checked for field dependence at several temperatures. A liquid sample of **4d** was condensed into a high purity quartz container on a vacuum line and the vessel backfilled with 0.5 atm of helium. The measured magnetic susceptibility (Fig. 5) exhibits a Curie tail due to the presence of trace amounts of paramagnetic material, likely trapped radicals in a diamagnetic host. The complete data are included in the Supplementary Materials.

Thermal stability. Pure, opaque black liquid radical **4d** (0.035 g, 0.15 mmol) was heated (250 °C) for three hours in a 5 mm o.d. NMR tube fitted with a break seal and wrapped in aluminium foil, giving a clear yellow liquid. ^{19}F NMR spectrum of the product, to which CCl$_3$F (0.055 g, 0.40 mmol) and SO$_2$ (0.58 g) were added: solution, δ [integration, assignment] 0 [0.34, CCl$_3$F], −55.5 and −56.2 [0.12, (CF$_3$CSSCCF$_3$)$_n$], −61.9/−62.2 unresolved (0.55, CF$_3$CNSNCCF$_3$ plus CF$_3$CSSCCF$_3$), assignments based on references 29 and 30.
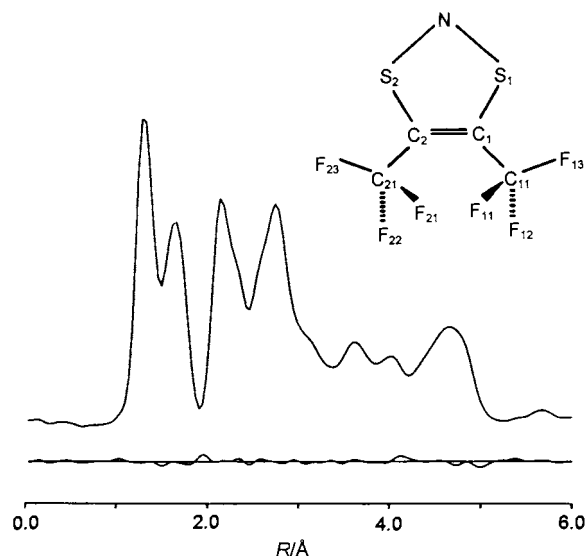

Fig. 6 Experimental radial distribution function for radical **4d** and difference curve.

86% of **4d** had decomposed to the observed products. Other results: % decomposition [temperature (time)]; 9 [23 °C (3 h)]; 16 [202 (2)]; 81 [209 (15)].

Photolytic stability. In a typical photolysis, pure opaque black liquid radical **4d** (0.18 g, 0.08 mmol) in a 5 mm o.d. NMR tube was exposed to direct sunlight for three hours giving a clear yellow liquid. SO$_2$ (0.60 g) and CCl$_3$F (0.069 g, 0.50 mmol) were added and flame sealed. ^{19}F NMR spectrum of photolysis products, to which CCl$_3$F (0.055 g, 0.40 mmol) and SO$_2$ (0.58 g) were added: δ (integration, assignment) 0 (0.55, CCl$_3$F), −55.5 and −56.2 (0.09, ([CF$_3$CSSCCF$_3$]$_n$), −61.9/−62.2 unresolved (0.36, CF$_3$CNSNCCF$_3$ and CF$_3$CSSCCF$_3$), assignments based on reference 29 and 30, corresponding to 85% decomposition.

Isolation and characterisation of CF$_3$CNSNCCF$_3$

The volatile materials (0.229 g) from the photolysis of pure radical **4d** (0.344 g, 1.43 mmol) were isolated in a U-tube trap at −196 °C, and melted to a pale yellow liquid at room temperature. A catalytic amount of N(CH$_3$)$_3$ (0.001g, 0.01 mmol) was added to polymerise the CF$_3$CSSCCF$_3$ (according to ref. 30), giving a non-volatile yellow solid and a volatile colourless liquid (0.10 g, 0.45 mmol, 31% yield based on **4d**) identified as pure CF$_3$CNSNCCF$_3$ by elemental analysis and comparison of the infrared, NMR and mass spectra with published spectra[29] (Found: C, 21.84; N, 11.50; S, 13.18%; M$^+$ *m/z* 222. C$_4$F$_6$N$_2$S requires C, 20.00; N, 12.61; S, 14.41%; M$^+$ *m/z* 222).

Electron diffraction of radical 4d

The electron diffraction intensities were recorded at two camera distances (25 and 50 cm) with a Balzers Gas Diffractograph KD-G2.[31] The accelerating voltage was about 60 kV and the electron wavelengths were calibrated with ZnO diffraction patterns. The sample, stainless steel inlet system and nozzle were at room temperature. The camera pressure during the experiment never exceeded 5 × 10^{-6} Torr. Two plates for each camera distance were analysed by the usual procedures.[32] The averaged molecular intensities $s \cdot M(s)$ in the s ranges 1.4–17 and 8–35 Å^{-1} in steps of $\Delta s = 0.2$ Å^{-1} are presented in the Supplementary Materials.

Analysis of the radial distribution function (Fig. 6) resulted in a preliminary model with a planar ring and the CF$_3$ groups in staggered positions with respect to the C=C double bond. The torsional position of the CF$_3$ groups correspond to that in *cis*-CF$_3$CH=CHCF$_3$.[33] In the least squares analyses a diagonal

Table 3 Structural parameters (values in Å and °)[a] for radical **4d** (gas phase)

C=C	1.324(7)	C=C–S[b]	114.8(3)
C–S	1.749(3)	C–S–N[b]	96.5(6)
S–N	1.634(2)	S–N–S	117.3(5)
C–C	1.481(3)	C=C–C	127.3(3)
C–F	1.330(2)	F–C–F	107.4(2)
		tilt[c]	1.5(6)

[a] Error limits are 3σ values and include a possible scale error of 0.1% for bond lengths. [b] Dependent parameter. [c] Tilt angle between C_3 axis of CF_3 group and C–C bond, away from C=C bond.

weight matrix was applied to the molecular intensities and scattering amplitudes and phases of reference 34 were used. Possible deviations of the ring conformation from planarity and of the CF_3 groups from the exactly staggered position were tested in a series of refinements. The agreement between model and experiment improves marginally for a slightly non-planar ring structure with an out-of-plane angle $\alpha \approx 5°$ (the angle between the S(1)NS(2) and S(1)C(1)C(2)S(2) planes, see Fig. 6). The agreement factors R increase for $\alpha > 10°$. This minor deviation from planarity should be interpreted in terms of a planar equilibrium configuration with a small out-of-plane vibrational amplitude. Torsional deviations of the CF_3 groups from the staggered positions up to 15° have no effect on the quality of the fit between experimental and calculated intensities. In the final analysis a planar ring and exactly staggered CF_3 groups (*i.e.* C_{2v} overall symmetry) were assumed. The CF_3 groups were constrained to C_{3v} symmetry with a possible tilt angle between the C_3 axes and the C–C bond directions. Assumptions for vibrational amplitudes are evident from Table 3 given in the Supplementary Materials. Nine independent geometric parameters and 14 vibrational amplitudes were refined simultaneously. The following correlation coefficients had values larger than |0.7|: C=C/CF, 0.83; C=C/FCF, 0.73 and CF/FCF, 0.84. The final results are summarized in Table 3.

Crystal structure determination

Growth of crystals for X-ray diffraction. A sample of radical **4d** held in a Pyrex capillary (o.d. 0.3 mm) was mounted on a Stoe Stadi diffractometer equipped with an Oxford Cryosystems low-temperature device.[35] It is usual in studies such as this to cool the sample, controlling the crystal growth front by careful adjustment of the temperature gradient. The rate of crystal growth can normally be observed visually, but here the intense colour of the sample made this impossible. The sample was therefore cooled through its melting point at various rates, and the crystallinity assessed at each stage from a rotation photograph. The results of most of these experiments were polycrystalline masses, but an indexable[36] diffraction pattern was obtained by cooling from 280 to 270 K at 20 K h^{-1}.

Crystal and data collection parameters. $C_4F_6NS_2$, $M = 240.17$. Triclinic, $a = 7.976(3)$, $b = 8.806(3)$, $c = 11.830(4)$ Å, $a = 102.15(2)$, $\beta = 93.40(2)$, $\gamma = 108.16(2)°$, $U = 764.8(4)$ Å^3 ($\lambda = 0.71073$ Å. $T = 220.0(2)$ K, space group $P\bar{1}$, graphite monochromated Mo-Kα radiation, $Z = 4$. Blue-black cylinder with radius 0.15 mm, $\mu = 0.752$ mm^{-1}. Reflections were measured with ω–θ scans; 5384 data were measured, of which 2697 were unique ($R_{int} = 0.0421$).

Structure solution and refinement. The structure was solved by Patterson methods (DIRDIF 96)[37] and refined against F^2 (SHELXTL).[38] All trifluoromethyl groups were rotationally disordered about their threefold axes. The refinement converged to a conventional R factor of 0.0404 [based on F and 1953 data with $F > 4\sigma(F)$], and $wR2 = 0.1085$ (based on F^2 and all 2690 data used during refinement). The final difference map extrema were 0.347 and -0.254 e Å^{-3}.

An attempt was made to collect data at 150 K but the peak profiles deteriorated significantly on cooling, possibly due to thermal stress or a nearby phase change, and so this experiment was abandoned.

CCDC reference number 186/2074.

See http://www.rsc.org/suppdata/dt/b0/b001489n/ for crystallographic files in .cif format.

Theoretical calculations

Initially UB3PW91/6-31G* geometry optimisations were carried out for radical **4d** and **3d** using the GAUSSIAN 94 suite of programs.[39] Subsequently geometry optimisations were completed using a different set of functionals and a basis set including diffuse functions (UMPW1PW91/6-31+G*) available in GAUSSIAN 98.[40] The starting geometries used for **3d** and **4d** were based on the electron diffraction results for the neutral **4d**. All optimised geometries were stationary points. Dimerisation and tetramerisation energies§ of **4d** were also calculated using MPW1PW91/6-31+G*; these were single point calculations using geometries taken from the crystal structure with the major occupancies of the disordered fluorine atoms (structure A in Fig. 8). Various possible dimers of **4a**, **4d**, and **4j** were also optimised at the UB3PW91/6-31G* level to access the dimerisation free energy, with the zero point energy and derived enthalpy corrections (to 298 K) taken from values calculated at the UB3PW91/3-21G* level. The optimised geometries and energies of **3d**, **4a**, **4d**, **4j**, **20a**, **20d**, **20j**, **21d**, **22a**, **22d**, **22j** and **24** are included in the Supplementary Materials. Vibrational frequencies for **4d** and **3d** were calculated at the same levels of theory and scaled by 0.96.[41] Unrestricted (U) and restricted open-shell (RO) DFT calculations were completed for the radical **4d** to assess Koopmans'-like orbital energies, together with UHF/6-31+G* and ROHF/6-31+G* Hartree–Fock calculations performed at the UMPW1PW91/6-31+G* geometry. In addition the first ionisation energy (IE) was calculated using an E(cation) $-$ E(radical) approach which has been shown to provide good first IEs for atoms[42] and molecules.[43] Both adiabatic (radical and cation optimised) and vertical (using optimised radical geometry for the cation) first IEs were obtained.

Chemistry of radical 4d

In a series of experiments, pure radical **4d** was treated with AsF_5, Cl_2, Br_2, I_2, O_2, H_2O, air, Hg, NO and Cu under different conditions. The experimental details, results of reactions, observations and product analyses are included in Table 4 and a more complete account is included in the Supplementary Materials.

Radical **4d** and AsF_5 gave **3d**[AsF_6] as clear colourless fibrous plates that are multiple crystals: $a = 6.908(3)$, $b = 24.483(10)$, $c = 7.182(3)$ Å, $a = 90$, $\beta = 108.28(3)$, $\gamma = 90°$, $V = 1153.5(9)$ Å^3.

3d[Cl]: orange moisture sensitive crystalline solid, mp 143–146 °C (Found: C, 18.00; Cl, 12.90; N, 5.21; S, 22.83%; M$^+$ m/z 240. $C_4ClF_6NS_2$ requires C, 17.43; Cl, 12.86; N, 5.08; S, 22.26%; M m/z 240). ^{19}F NMR (SO$_2$, CCl$_3$F): δ 0 (CCl$_3$F) and 52.8 (6F, S, [CF$_3$ĊSNSĊCF$_3$]$^+$). IR spectrum [Nujol or fluorolube mull, KBr plates]: 1511w, 1314m, 1246ms, 1193s, 1177s, 1078m, 1002w, 944w, 880w, 784w, 759m, 736m, 711m, 609w, 583w, 465w and 410m cm^{-1}. Mass spectrum [direct inlet, 25 °C, 70 eV]: m/z (% of highest peak, assignment) 240 (100, [CF$_3$-ĊSNSĊCF$_3$]$^+$), 226 (60, [CF$_3$ĊSSĊCF$_3$]$^+$), 221 (48, [CF$_3$-ĊSNSĊCF$_2$]$^+$), 194 (24, [CF$_3$CSCCF$_3$]$^+$), 162 (20, [CF$_3$C-CCF$_3$]$^+$), 126 (32, [CF$_3$C$_2$S]$^+$), 113 (43, [CF$_3$CS]$^+$), 106 (28, [SNSCO]$^+$), 93 (20, [CF$_3$C$_2$]$^+$), 88 (28, unassigned), 78 (100,

---

§ It was assumed that the dimerisation or tetramerisation energy was the difference in the calculated total energy of the dimer or tetramer minus two or four times the calculated total energy of the monomer.

Table 4 The chemistry of radical 4d

4d (g, mmol)	Reagent (g, mmol)	Solvent (g)	Procedure [a]	Colour changes [b]	Apparent reaction time [c]	Product(s) (g, mmol, % yield)
0.050, 0.21	AsF_5 (0.100, 0.59)	SO_2 (2.36)	A	Opaque black ⟶ clear colourless	<1 min	Soluble white solid, 3d[AsF_6] (0.090, 0.21, 100)
0.108, 0.45	Cl_2 (0.257, 3.63)	SO_2 (0.72)	A	Opaque black ⟶ light yellow	<1 min	Soluble orange solid, 3d[Cl][d] (0.111, 0.40, 90)
0.182, 0.76	Br_2 (0.733, 4.58)	CH_2Cl_2 (2.72)	A	Opaque black ⟶ dark red	<1 min	Soluble red-black solid, 3d[Br][d] (0.236, 0.74, 97)
0.490, 2.20	I_2 (0.262, 1.04)	SO_2 (7.08)	A	Opaque black	28 h	4d (0.38, 1.62, 80), no reaction
0.019, 0.08	O_2 (0.096, 3.0)	—	B	Unknown	<1 min	A complex non-volatile mixture
0.008, 0.034	O_2 (0.0018, 0.11)	CCl_3F (48.02)	C	Very light blue	6 h	4d (ESR), no reaction
0.044, 0.18	O_2 (0.0038, 0.24)	SO_2 (0.44)	D	Opaque black ⟶ clear yellow	<1 min[e]	A complex mixture of greater than 10 diamagnetic products (^{19}F NMR)
0.060, 0.25	Water (0.017, 0.93)	CH_2Cl_2 (0.67)	D	Opaque black ⟶ opaque black (ppt.)	20 h	A complex mixture of greater than 30 diamagnetic products (^{19}F NMR)
0.024, 0.10	Air	CH_2Cl_2 (0.75)	D	Opaque black ⟶ yellow	1 h	A complex mixture of greater than 30 diamagnetic products (^{19}F NMR)
0.178, 0.74	NO (0.087, 2.90)	CCl_3F (0.98)	A	Opaque black	20 h	4d (0.010, 0.043, 6), no reaction
0.085, 0.35	Cu^f (0.330, 5.16)	SO_2 (3.94)	A	Opaque black	20 h	4d (0.078 g, 0.32, 91), no reaction

[a] A: Reaction between a solution of radical 4d and reagent in a two-bulb vessel. B: Reaction between gaseous 4d and O_2 in an infrared cell. C: Reaction between gaseous 4d and reagent in a two-bulb vessel. The addition of each aliquot was made at room temperature and each chamber was washed several times with the solvent. The addition of each aliquot of O_2 (0.01, 0.02, 0.04 and 0.04 mmol) isolated in side arms attached to a bulb containing 48 g CCl_3F and 0.034 mmol 4d above before the addition of the next aliquot. D: Reaction between a solution of 4d and reagent in a 5 mm o.d. thick walled NMR tube. The reaction vessel was repeatedly inverted to ensure good mixing before the ESR spectrum was obtained in situ after standing for one hour. The reaction mixture was allowed to stand for one hour before the addition of the next aliquot. The addition of O_2 was made by expanding gaseous O_2 into the tube at −196 °C. The addition of water was made by syringe through a static layer of N_2. The addition of air was made by exposure of the solution to room air for one hour. [b] Of the solution. [c] The apparent reaction times estimated from colour changes or the duration of the experiment. [d] The product was purified by sublimation in a static vacuum at 80 °C. [e] A strongly exothermic reaction was observed upon warming to r.t. [f] The powdered Cu was flame dried under vacuum prior to use. Although the masses indicate that no reaction occurred, the initially bright metal surface was coated with a black insoluble solid after the reaction.

[SNS]$^+$), 75 (16, unassigned), 69 (80, [CF_3]$^+$), 64 (30, S_2^+), 46 (88, [NS]$^+$), 44 (16, [CS]$^+$), 37 (8, ^{37}Cl$^+$), 35 (20, ^{35}Cl$^+$), 32 (80, S^+) and 28 (100, N_2^+). Peaks greater than 5% included. This compound was also prepared in lower yield from the reaction of 3d[AsF_6] (0.420 g, 1.00 mmol) and KCl (0.075 g, 1.00 mmol) in 3.128 g SO_2. The orange crystalline product (0.174 g, 0.63 mmol, 63% yield) was recovered by sublimation from the non-volatile reaction residue.

3d[Br]: air stable (IR) red-black crystalline solid, mp 135–136 °C (Found: C, 14.92; Br, 24.89; N, 4.33; S, 19.00%; M^+ *m/z* 240. $C_4F_6NS_2$ requires C, 15.01; Br, 24.96; N, 4.38; S, 20.03%; M^+ *m/z* 240). ^{19}F NMR (SO_2, CCl_3F): δ 0 (CCl_3F) and −53.4 (6F, S, [$CF_3CSNSCCF_3$]$^+$). IR spectrum [Nujol or fluorolube mull, KBr plates]: 1510m 1304ms, 1284w, 1259s, 1185vs, 1070m, 982w, 930m, 876w, 772m, 730m, 709ms, 608ms, 578m, 460m and 405m cm^{-1}. Mass spectrum [direct inlet, 25 °C, 70 eV]: *m/z* (% of highest peak, assignment) 240 (50, [CF_3-$CSNSCCF_3$]$^+$), 221 (50, [$CF_3CSNSCCF_2$]$^+$), 162 (24, [CF_3-$CCCF_3$]$^+$), 126 (37, [CF_3C_2S]$^+$), 113 (35, [CF_3CS]$^+$), 106 (22, [SNSCO]$^+$), 93 (12, [CF_3C_2]$^+$), 80 (28, [S_2O]$^+$[?]), 78 (75, [SNS]$^+$), 69 (80, [CF_3]$^+$), 46 (80, [NS]$^+$), 32 (24, S^+) and 28 (100, N_2^+). Peaks greater than 5% included. This compound was also quantitatively prepared from the reaction of 3d[AsF_6] (0.86 g, 2.05 mmol) and KBr (0.30 g, 2.52 mmol) in 5.50 g SO_2. The red-black crystalline solid (0.60 g, 1.88 mmol, 94% yield) was recovered by sublimation from the non-volatile reaction residue.

The reduction of [R^{1}CSNSCR^2][AsF$_6$]

In a series of experiments, [R^{1}CSNSCR^2][AsF_6] (approximately 2–3 mg) was mixed with either $Na_2S_2O_4$ and [N(CH_3)$_4$][Cl] (approximately 3 mg each) or (C_6H_5)$_3$Sb and [N(CH_3)$_4$][Cl] (approximately 3 mg each) in a quartz 3 mm o.d. ESR tube. The solvent [SO_2 and CCl_3F in a 1:4 w/w ratio] was condensed onto the mixture [to give a solution of approximately 10^{-4} M concentration], which was shaken at room temperature for one minute. The ESR spectra of these solutions were then acquired as a function of time. The results of these reactions are given in Table 5. Preparative scale reactions are also included for comparison.

The generation and decomposition of [HCSNSCCF$_3$] 4c

Sulfur dioxide (3.70 g) was condensed onto [HCSNSCCF$_3$][AsF_6] (3c[AsF_6]) (0.350 g, 1.00 mmol), (C_6H_5)$_3$Sb (0.353 g, 1.00 mmol) and [N(CH_3)$_4$][Cl] (0.258 g, 2.30 mmol) giving an opaque black solution on rapidly warming to r.t. with shaking for one minute. The volatile materials were collected in a U-tube trap (−196 °C) by dynamic vacuum leaving a brown-black tar. The former (a white solid [presumably SO_2] and a blue-black crystalline solid [presumably 4c]) gave a black solution at r.t. changing to brown-black after one hour. Removal of the volatile material [SO_2; infrared] gave a non-volatile brown tarry solid, which was recovered and heated (80 °C under vacuum) to give a non-sublimed brown solid and a sublimed purple-black crystalline solid that was identified as SCSNSCCF$_3$ (0.025 g, 0.12 mmol, 12% yield) by comparison with data reported for related compounds.[44]

SCSNSCCF$_3$, 13: mp 104–106 °C. IR spectrum [Nujol mull, KBr plates]: 1494w, 1340w, 1295m, 1282w, 1267m, 1222w, 1208w, 1176m, 1151m, 1082w, 978m, 939m, 897w, 823vw, 773sh, 755sh, 743sh, 728m, 692w, 438w, 400w and 360w cm^{-1}. ^{19}F NMR: δ (integration, assignment) 0.0 (0.74, CCl_3F) and −59.8 in SO_2 solution (0.26, [SCSNSCCF$_3$]). Mass spectrum [direct inlet, 25 °C, 70 eV]: *m/z* (% of highest peak, assignment) 203 (14, [$CF_3CSNSCS$]$^+$), 157 (15, [CF_3CSSC]$^+$), 113 (12, [CF_3CS]$^+$), 88 (6, [CSSC]$^+$), 78 (5, [SNS]$^+$), 32 (23, S^+) and 28 (100, N_2^+). Peaks greater than 5% included.

Table 5 The reduction of [R¹$\overline{CSNSC}$R²][AsF₆] in dilute solution

R¹	R²	Reduction mixture	g	a^{N14}/mT	Additional couplings (mT)	Apparent half-life (h)[a]
H	H	[b]	2.007	1.07	$a^H = 0.13$	<1[c]
H	CH₃	[b]	2.006	1.07	$a^H = 0.14$	[d]
H	CF₃	[e]	2.009	1.10	$a^H = a^F = 0.075$	0.3
CF₃	CF₃	[e]	2.005	1.13	$a^F = 0.069$	>200
H	CN	[e]	2.004	1.07	[f]	>0.1
Si(CH₃)₃	Si(CH₃)₃	[e]	2.008	1.10	[f]	0.5[g]
CO₂CH₃	CO₂CH₃	[e]	2.006	1.08	[f]	>200[h]

[a] Determined from the change in intensity of the ESR signal *i.e.* the time required for intensity to diminish by half assuming the signal width is constant. [b] Reduction with Na₂S₂O₄ in C₄H₄O (THF). [c] When 1.01 mmol of **3a**[AsF₆] was stirred with 2.81 mmol of Na₂S₂O₄ in SO₂ (2.38 g) at room temperature for one month the starting materials were recovered unchanged (IR). An immediate reaction of 5.59 mmol of **3a**[AsF₆] with 5.59 mmol of Sb(C₆H₄)₃ and 5.59 mmol of N(CH₃)₄Cl in 8.38 g of SO₂ was observed that gave an opaque red-black solution over an insoluble black solid. The soluble brown solid was shown to contain [N(CH₃)₄][AsF₆], Sb(C₆H₅)₃Cl₂ and Sb(C₆H₅)₃ by IR The insoluble black solid was washed with liquid SO₂ for a month to remove soluble impurities and the remaining black solid (0.315 g) characterised by IR [(Nujol mull, KBr plates); 1201s, br, 1090ms, 1040w, sh, 1025s, 870m, 775w, 683w, 603m, 561w, 540w cm⁻¹] and elemental analyses (Found: C, 17.50; H, 1.93; N, 7.91; S, 48.74. C₂H₂NS₂ requires C, 23.06; H, 1.94; N, 13.45; S, 61.55%). For complete experimental details see reference 25. [d] When 1.00 mmol of **3b**[AsF₆] was stirred with 3.00 mmol of Na₂S₂O₄ in SO₂ (2.94 g) at room temperature for one month the starting materials were recovered unchanged (IR). [e] Reduction with [N(CH₃)₄][Cl] and SbPh₃ and in SO₂ solvent. [f] No secondary hyperfine couplings were observed. [g] Reaction of 0.53 mmol of **3e**[AsF₆] with 2.50 mmol of Na₂S₂O₄ in 3.73 g of SO₂ gave an opaque purple-red solution after 24 hours. The IR spectrum of the insoluble black solid gave only bands assigned to Na₂S₂O₄. The soluble materials formed an intractable black tar. [h] Reaction of 0.55 mmol of **3f**[AsF₆] with 1.97 mmol of Na₂S₂O₄ in 2.50 g of SO₂ gave an opaque brown-black solution after 36 hours. The IR spectrum of the insoluble black solid gave only bands assigned to Na₂S₂O₄ and **3f**[AsF₆]. The soluble materials formed an intractable brown tar.
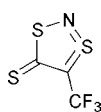
13

¹⁹F NMR analysis of the reduction of 3c[AsF₆]

SO₂ (0.70 g) and CCl₃F (0.068 g, 0.50 mmol) were added to **3c**[AsF₆] (0.036 g, 0.10 mmol), (C₆H₅)₃Sb (0.036 g, 0.10 mmol) and [N(CH₃)₄][Cl] (0.037 g, 0.30 mmol) in a 5 mm o.d. NMR tube. The reaction mixture was warmed to room temperature and shaken for one minute. The ¹⁹F NMR spectra of the initial solution contained only resonances assignable to CCl₃F and [AsF₆]⁻ (δ −56.8, $J_{As-F} = 921$ Hz) consistent with quantitative reduction of **3c** to the radical. After twenty minutes there were 15 unassigned resonances with a total integrated intensity equal to that of the original **3c**, which can be found in reference 25.

The generation of radical 4c and reaction with chlorine

Sulfur dioxide (3.70 g) was condensed onto **3c**[AsF₆] (0.143 g, 0.40 mmol), (C₆H₅)₃Sb (0.173 g, 0.50 mmol) and [N(CH₃)₄][Cl] (0.110 g, 1.00 mmol) in one bulb of a two bulb, two valve vessel, rapidly warmed to r.t. and shaken for one minute, giving an opaque black solution. The volatile materials were collected in a U-tube trap (−196 °C) by dynamic vacuum leaving a brown-black tar. The former (a white solid [presumably SO₂] and a blue-black crystalline solid [presumably **4c**]) were treated immediately with Cl₂ (0.212 g, 3.00 mmol). The initially opaque black solution changed to a clear yellow in less than thirty seconds. The volatile materials [SO₂ and SO₂Cl₂; infrared] were removed to give a waxy yellow non-crystalline solid, which was recovered and identified as **3c**[Cl] (0.30 g, 0.15 mmol, 36% yield). The product decomposed to a black tar on attempted *in vacuo* sublimations at 70 °C. ¹H NMR: δ (integration, assignment) 11.2 (0.95, [H$\overline{CSNSC}$CF₃]⁺), 3.14 (< 0.03, impurity) and 1.25 (< 0.03, impurity). ¹⁹F NMR in SO₂: δ (integration, assignment) 0.0 (0.30, [CCl₃F]), −53.6 (0.60, [H$\overline{CSNSC}$CF₃]⁺) and −56.7 (0.10, impurity). Assignments of [H$\overline{CSNSC}$CF₃]⁺ resonances were based on comparison of spectra from solutions of [H$\overline{CSNSC}$CF₃][AsF₆] in SO₂ (this work). IR spectrum [Nujol mull, KBr plates]: 3075w, 1280ms, 1260m, 1192s, 1158vs, 1039w, 990w, 955w, 857m, 776ms, 730m, 679m, 630w, 580w, 550w and 409m cm⁻¹.

Discussion

Preparation of 4d

A typical preparative scale reduction of **3d**[AsF₆] in liquid sulfur dioxide used sodium dithionite Na₂S₂O₄ in large excess as the reducing agent according to eqn. (3). This chemical reaction

$$Na_2S_2O_4 + 2\ \mathbf{3d}[AsF_6] \longrightarrow$$
$$2\ \mathbf{4d} + 2\ SO_2 + 2\ Na[AsF_6] \quad (3)$$
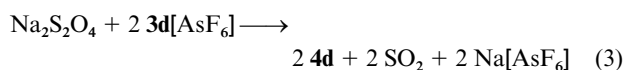
was preferred because the oxidised product is the solvent SO₂ and the spectator ions precipitate as an insoluble, non-volatile ionic salt. The relatively low purity of the reducing agent [*ca.* 85% reported by the supplier[45]] apparently did not result in contaminating volatile or soluble impurities. Preparative scale reductions were also observed from the reactions of the hexafluoroarsenate salt **3d**[AsF₆] with KI, or a mixture of triphenylantimony and tetramethylammonium chloride (Table 1).¶ This radical could be prepared in the absence of solvent by the reaction of the chloride salt of **3d** with triphenylantimony by mildly heating the mixture under vacuum in the dark according to eqn. (4). However, this route required the preparation of

$$2\ \mathbf{3d}[Cl] + Sb(C_6H_5)_3 \longrightarrow 2\ \mathbf{4d} + Sb(C_6H_5)_3Cl_2 \quad (4)$$
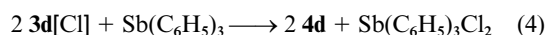
the intermediate chloride salt from the metathetical ion exchange reaction between **3d**[AsF₆] and tetramethylammonium chloride.

The radical **4d** was isolated from these reaction mixtures by a fractional distillation train of sequential U-tube traps and isolated as a black crystalline solid in the −15 °C trap. It is very reactive towards moisture and oxygen and very photochemically sensitive (see below), leading to some loss of sample during preparation and purification. Without these difficulties the yield would be close to 100% (observed isolated yield: 82% total mass product in Table 1). To obtain very pure samples for analysis it was usually necessary to repeat the fractional distillation three times and store the material in the dark to minimise photolytic decomposition. The purity of the radical **4d** was routinely determined by a combination of infrared (sensitive to the presence of SO₂ solvent and photolytic impurities) and ¹⁹F

¶ **4d** was also generated *in situ* as one of the products of the reaction of **3d**[AsF₆] with CsN₃ in SO₂.[46]

NMR spectroscopy (sensitive to the presence of photolytic decomposition products). The purity of a routine sample was greater than 95% by integration analysis of the ^{19}F NMR spectra against an internal concentration standard. The absolute composition of the product was confirmed by good elemental analyses.

The thermal and photochemical dissociation of radical 4d

The pure radical in the gas phase and in hexane solutions [4.5×10^{-2} M] was shown to be unstable with respect to irreversible decomposition by photochemical (daylight) and thermal processes ($T_{\text{decomp}} = 209\,°C$, % decomp. = 81 after 15 hours). The product by either thermal or photochemical decomposition was a diamagnetic yellow oil that contained (14 and 15; or known oligomers of 15) in exactly the same stoichiometric ratios [^{19}F NMR]. Reduction of 7d gives 16,[9] which decomposes to 15 and its oligomers.[30] Therefore we propose that 4d thermally and photochemically decomposes ($\Delta H_{\text{rxn}} = -429$ kJ)‖, according to Scheme 2 with subsequent decomposition of 16 to 15 and elemental sulfur.
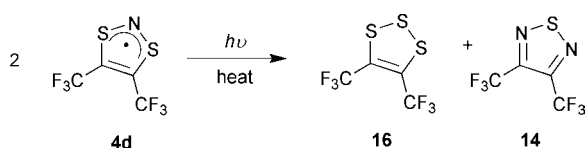
Scheme 2
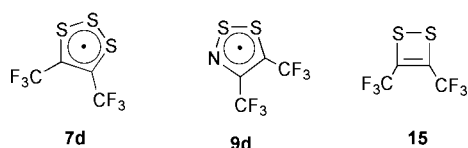
Similar switching of sulfur and nitrogen positions occurs within the ring on the rearrangement of radical 1 to 2. We have shown that this occurs *via* a photochemically symmetry-allowed rearrangement of the dimer of 1 to the dimer of 2 by minimal atomic displacement.[11,12] A similar rearrangement of a dimer of 4d to the observed products is not readily envisaged. However, it is tempting to suggest that the dimer of 4d rearranges to 14 and 16 (*via* 9d?)[48] and hence to 14 and 15. Aromatic and aliphatic derivatives of the anions of sulfur diimides RN=S=NR are known to be unstable with respect to rearrangement (ref. 1e and references therein). No evidence for dimer formation of 4d was evident from a quantitative ESR study in solution as a function of temperature. We propose that the decomposition occurs *via* an excited state of 4d either produced photochemically or thermally, the mechanism of which warrants further study.

The characterisation and physical properties of radical 4d

A pure sample of the isolated radical in an evacuated vessel at room temperature was a black liquid (mp = 11 °C) [black in reflected light and greenish with transmitted light through a thin film] under a highly visible blue vapour (measured vapour pressure at r.t. = 25 mmHg). A similar blue colouration was observed in dilute solutions of the radical in non-polar solvents such as hexane and Freon-11 while solutions in SO_2 were greenish brown possibly due to formation of a weak charge transfer complex $4d\cdot SO_2$.

‖ The calculation of the enthalpy of reaction based on a simple Hess's Law analysis using bond dissociation energies E[47] and the assumption that the π delocalisation energies of the two heterocycles are the same [$\Delta H_{\text{rxn}} = E_{\text{broken}}[4E_{\text{S-N}}$ (145 kJ)] $- E_{\text{formed}}[2E_{\text{S-S}}(236$ kJ) $+ 2E_{\text{S-N}}$ (145 kJ)].

The density in the liquid state (1.63 g cm^{-3} at 22 °C) is approximately 20% less than in the solid (1.97 g cm^{-3} at -78 °C). Normal density changes on melting are about 4%, although those for the smaller inert gases are comparable and are attributed to changes in overall structure of the material on change of phase.[49] We attribute the change in density to a change from a diamagnetic tetramer (see below) in the solid to a paramagnetic liquid containing isolated molecules separated by the sums of the corresponding van der Waals radii. In the solid state the monomers are joined by weak S···S π*–π* bonds perpendicular to the rings (average 3.14 Å). An expansion of the distance between the rings to 3.7 Å (the anisotropic van der Waals radii of S perpendicular to the ring estimated as 2.03 Å [50]) would account for the change in density. A large change in density on melting is likely to be a distinguishing characteristic of *the paramagnetic liquids*.

The vapour pressure of the black solid and liquid phases of the radical 4d was measured over a range of temperatures ($-20 < T < 100$ °C). The extrapolated value for the boiling point of the radical was 119 °C. The data are consistent with the following thermodynamic values for pure 4d: $\Delta H_{\text{vap}} = 38.1 \pm 0.5$ kJ mol^{-1}, $\Delta S_{\text{vap}} = 97.1 \pm 1.0$ J K^{-1} mol^{-1}; $\Delta H_{\text{sub}} = 49.0 \pm 1.5$ kJ mol^{-1}, $\Delta S_{\text{sub}} = 172.1 \pm 2.0$ J K^{-1} mol^{-1}; $\Delta H_{\text{fus}} = 10.8 \pm 1.5$ kJ mol^{-1}, $\Delta S_{\text{fus}} = 75.3 \pm 3.0$ J K^{-1} mol^{-1}. The values for ΔH_{vap} and ΔH_{sub} were determined directly from experimental data whilst ΔH_{fus} was calculated using the assumption that the heat of sublimation is equal to the sum of the heats of fusion and vaporisation. This derived value for the enthalpy of fusion was confirmed by direct measurement using Differential Scanning Calorimetry which measured the value of $\Delta H_{\text{fus}} = 11.5 \pm 0.1$ kJ mol^{-1}.[51,52] Comparison of the physical data with those reported for *cis*-2,3-dichloro-1,1,1,4,4,4-hexafluoro-2-butene ($\Delta H_{\text{vap}} = 32.6$ kJ mol^{-1}) and related compounds [included in the Supplemental Materials] shows that 4d behaves very much like a molecular, covalent compound in the solid, liquid and gas phase (Troutons Rule, $\Delta H_{\text{vap}}/T_{\text{bp}} = 88$ J K^{-1} mol^{-1}; 4d, $\Delta H_{\text{vap}}/T_{\text{bp}} = 97$ J K^{-1} mol^{-1}), with a low dipole moment of 0.1 (UB3PW91/6-31G*) and 0.4 Debye (UMPW1PW91/6-31+G*). It is as though the energy on changes of state is the same as if 4d were not a radical, *i.e.* the energy of intermolecular interaction between unpaired electrons is minimal. Consistently 4d has no tendency to associate as revealed by variable temperature ESR in CCl$_3$F, and the calculated (MPW1PW91/6-31+G*) energy of formation of the tetramer from four monomers in the gas phase is 33 kJ mol^{-1} per tetramer. Given the method of calculation we can conclude that the tetramerisation energy is very small.

The magnetic properties of radical 4d

The pure radical 4d is paramagnetic in the liquid ($\mu_{\text{eff}} = 1.53\ \mu_B$, 22 °C) and diamagnetic in the solid state ($\mu_{\text{eff}} = 0\ \mu_B$, 0 °C) by magnetic susceptibility measurements (Gouy method). This magnetic behaviour was confirmed by quantitative, dual cavity, variable temperature ESR spectroscopy and variable temperature magnetic susceptibility (Figs. 4 and 5). The ESR experiment reveals that the solid material has approximately thirty times less unpaired spins than the liquid at 296 K in CCl$_3$F and neat liquid 4d had no tendency to form diamagnetic dimers or polymers. The variable temperature magnetic susceptibility measurements [Faraday method, Fig. 5] reveal that the diamagnetic solid [χ_m* (140 K) = -25.7×10^{-6} cgs] became a paramagnetic liquid [χ_m* (286 K) = $+835 \times 10^{-6}$ cgs] upon melting. This material was the first compound to be shown to have such profoundly different magnetic properties in the solid and liquid states making 4d the first *Paramagnetic Liquid*. Subsequently research has discovered other paramagnetic liquids including the trifluoromethyl and tertiary butyl derivatives of the 1,3,2,4-dithiadiazolyl 1 and 1,2,3,5-dithiadiazolyl 2 radicals.[12] There are examples of paramagnetic solids, *e.g.* the

related 1,3,2-dithiazolyl radicals fused to aromatic systems, *e.g.* **17** and **18**, and related multiradicals.[21] A recent report of **18**[21d] suggested that these radicals could be applied in thermal sensors, switching units, and information storage media.
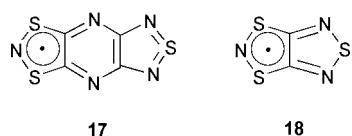
The concentration of unpaired spins in a 4.3 M solution of radical **4d** in CCl$_3$F over the temperature range from 226 to 318 K does not change as measured by dual cavity, quantitative ESR spectroscopy, revealing that there is no measurable tendency to dimerise or polymerise in solution. Related radicals have small solution dimerisation energies ([RC̄NSSN] **2**: R = C$_6$H$_5$, $\Delta H_{dimerisation}$ = −37 kJ mol^{-1}; R = CF$_3$, $\Delta H_{dimerisation}$ = −37 kJ mol^{-1}; R = *t*-C$_4$H$_9$, $\Delta H_{dimerisation}$ = −31 kJ mol^{-1} Ph C̄SNSNS, $\Delta H_{dimerisation}$ = −19.0 (2) kJ mol^{-1}).[22,52,53] If the same π*–π* spin-paired dimer **19d** were to form in solution as is observed in the solid state (one half of the tetramer shown in Fig. 7] then the dimerisation would be hindered by electrostatic repulsion between the relatively highly charged adjacent atoms.** Consistently the dimer **19d** is not a stationary point on the potential hypersurface (UB3PW91/6-31G*, starting from X-ray geometry). If a tetramer similar to that in the solid state were formed it would be heavily disfavoured by entropy. The most favourable σ bonded dimer is the N–N bonded dimer **20d** (N–N distance 1.427 Å), with a gas phase dimerisation enthalpy of −13.6 kJ mol^{-1}, and ΔG (dimerisation) of 52.1 kJ mol^{-1} (UB3PW91/6-31G* optimised geometry and atomic charges included in the Supplemental Materials).

19,20,21   R =
a   H
d   CF$_3$
j   CH$_3$
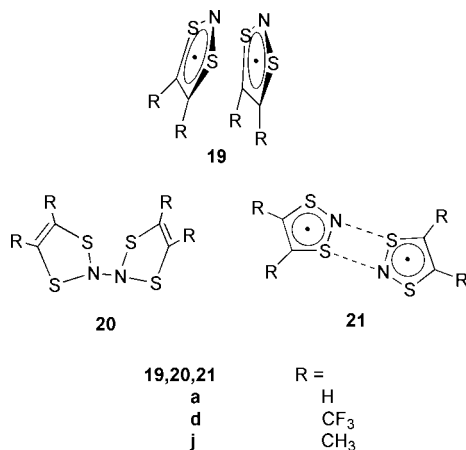
In solution the radical has an extrapolated value for the magnetic moment of 1.9 μ_B at infinite dilution (Gouy method). Similar changes in magnetic moment on change of concentration have been observed in the related paramagnetic liquid [(CH$_3$)$_3$CC̄NSSN·] **2** (R = C(CH$_3$)$_3$). The lower magnetic moment of the neat liquid [μ = 1.43 μ_B] is consistent with the presence of long-range weak intramolecular antiferromagnetic interactions. Similar values of the room temperature magnetic moments are found for the paramagnetic solids **7d**[AsF$_6$][9] and [CF$_3$C̄SSSN][AsF$_6$].[10] The magnetic moment of the liquid **4d** decreases with an increase of temperature above the melting

---

** The atomic charges are very dependent on the basis set and the method by which the charges are deduced. For radical **4d**, Mulliken (UB3PW91/6-31G*)/Mulliken (UMPW1PW91/6-31 + G*)/NBO charges: N (−0.766/−0.429/−0.846), S(0.636/0.431/0.706), in plane C (−0.336/−0.480/−0.340), exocyclic C (1.293/1.075/1.093), F (av.) (−0.404/−0.271/−0.346).

Table 6 Selected bond lengths [Å] and angles [°] for radical **4d** in the solid phase

| S(1)–N(2)	1.646(3)	S(6)–N(7)	1.638(3)
S(1)–C(5)	1.730(3)	S(6)–C(10)	1.737(3)
N(2)–S(3)	1.640(3)	N(7)–S(8)	1.639(3)
S(3)–C(4)	1.740(3)	S(8)–C(9)	1.734(3)
C(4)–C(5)	1.351(5)	C(9)–C(10)	1.349(4)
C(4)–C(41)	1.493(5)	C(9)–C(91)	1.503(4)
C(5)–C(51)	1.495(5)	C(10)–C(101)	1.490(5)
N(2)–S(1)–C(5)	98.79(15)	N(7)–S(6)–C(10)	98.47(15)
S(3)–N(2)–S(1)	114.47(16)	S(6)–N(7)–S(8)	114.69(17)
N(2)–S(3)–C(4)	98.57(15)	N(7)–S(8)–C(9)	98.72(15)
C(5)–C(4)–C(41)	128.2(3)	C(10)–C(9)–C(91)	128.0(3)
C(5)–C(4)–S(3)	114.0(2)	C(10)–C(9)–S(8)	113.8(2)
C(41)–C(4)–S(3)	117.7(2)	C(91)–C(9)–S(8)	118.2(2)
C(4)–C(5)–C(51)	127.5(3)	C(9)–C(10)–C(101)	127.9(3)
C(4)–C(5)–S(1)	114.0(2)	C(9)–C(10)–S(6)	114.1(3)
C(51)–C(5)–S(1)	118.5(3)	C(101)–C(10)–S(6)	117.9(3)
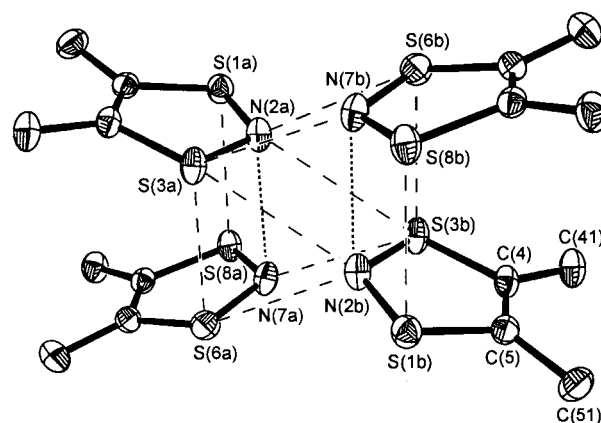
Fig. 7 An ORTEP[54] drawing of the solid state tetramer of radical **4d**. Fluorine atoms have been omitted for clarity. The thermal parameters are drawn at 30% probability.

point [Fig. 5] showing that the decrease is not due to dimer [or tetramer] formation and strongly implies that the liquid consists of essentially isolated monomer radicals separated by the sums of the corresponding van der Waals radii. This thesis is also supported by the large change of volume on melting.

The structure of radical 4d in the gas and solid phases as determined by electron diffraction and X-ray crystallography

The high vapour pressure (25 mmHg at r.t.) and stability of the radical **4d** allow structural determination in the gaseous and solid state. The gas phase electron diffraction structure [Table 3 and Fig. 6] and the crystal structure [Table 6, Figs. 7 and 8] were determined and the structure of **4d** and the corresponding **3d** determined by *ab initio* theoretical calculations. The data for the discrete molecules are compared in Table 7. The crystal structure of **4d** was originally determined by Englert *et al.*[55] but the accuracy was low and a dimer was identified and published in a Ph.D. thesis by one of us [M. J. S.].[25] This dimer was reported in a review[1a] and incorrectly attributed to our preliminary communication.[22a] In this work the crystal structure was redetermined at much higher accuracy and shown to be a tetramer, not a dimer as previously reported.

The structures of the two crystallographically independent planar **4d** monomers in the solid state are essentially identical. At 220 K the CF$_3$ groups are not freely rotating, and the crystallographic data are consistent with both the major and minor sets of fluorine atoms arranged such that each set of CF$_3$ groups within each monomer are geared, as shown in Fig 8 (A) and (B). The ESR of the matrix-isolated **4d** has been analysed by Mattar[56] and the fluorines shown to be magnetically non-equivalent, consistent with the geared geometry. In the gas
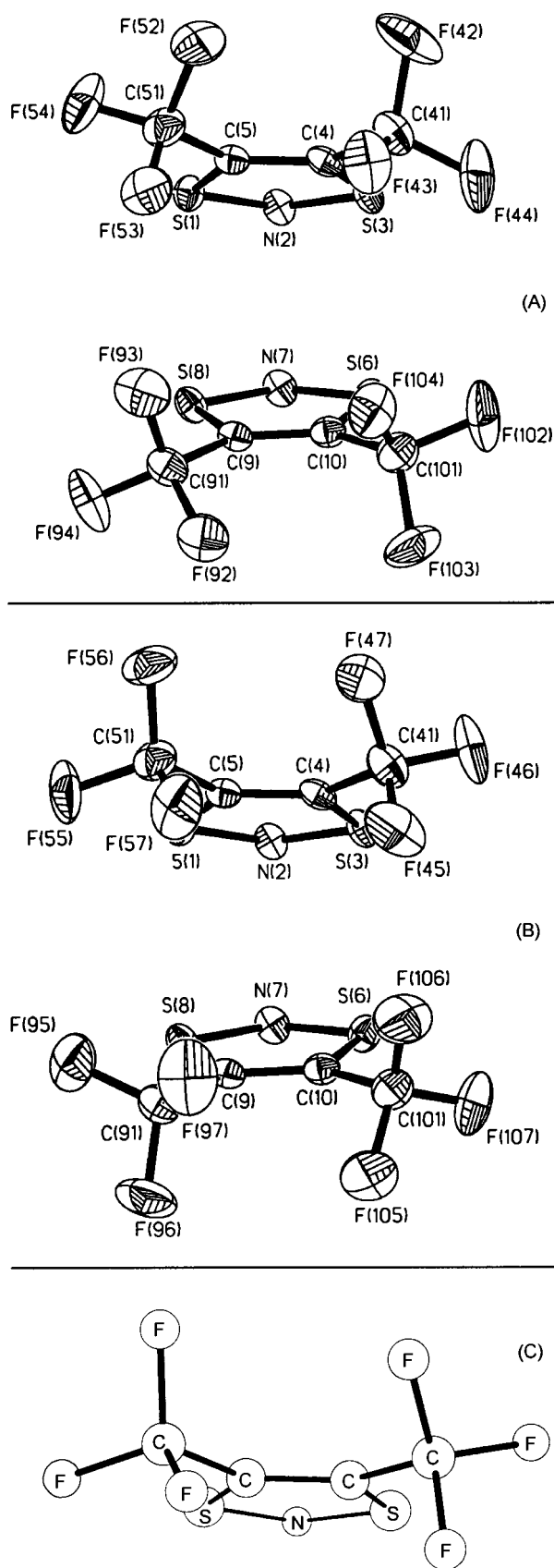
Fig. 8 ORTEP diagrams of the two independent monomers of radical **4d**, showing the orientation of the major (A) and minor (B) occupancies of the disordered fluorine atoms of the CF₃ groups, compared to the calculated structure (C). The thermal parameters are drawn at 30% probability.

phase the electron diffraction data are consistent with the CF$_3$ groups arranged in a staggered orientation with respect to the C=C bond with overall C_{2v} molecular symmetry in the final

refinement. However the fit of electron diffraction intensities is not significantly changed with the CF$_3$ groups in geared positions. Energy barriers to rotations are low and there is nearly free rotation of CF$_3$ groups in the gas phase. The orientation of the CF$_3$ groups in the calculated optimised geometry of **4d** is almost identical to that in the monomer (Fig. 8).

The structures of the 1,3,2-dithiazolyl radicals **4d**, **4h**, and **5** [Table 7] do not reveal any crystallographically significant differences in bond length within the heterocyclic rings, with the exception of the C–C bond. In **4d** the C–C bond length [1.351(5) Å] is consistent with that expected for an sp²–sp² olefin [1.36 Å]. The same bond is significantly longer in the radicals **4h** and **5** due to π bond delocalisation to the substituent [**4h**, CN; **5**, fused aromatic ring] which acts to lower the relative bond order from that in radical **4d**.

The bond distances of radical **4d** and the corresponding cation **3d** (Table 7) are consistent with the nature of the calculated SOMO of **4d**, *i.e.* S–N and C–S lengthen and C–C shortens on addition of an electron to **3d** as previously discussed.[20]

SOMO of **4d**
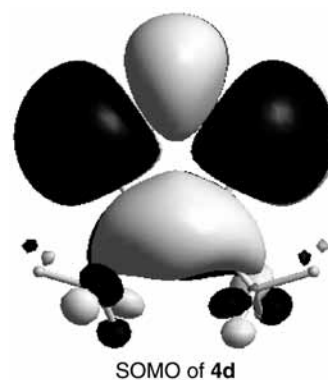
Radical **4d** is planar in both the gaseous and solid phases, and taking into account that there can be systematic differences of ± 0.03 Å and ± 3° between values obtained from ED and X-ray diffraction,[57] the structures of the ring are essentially identical in both phases (see Table 7). This is supported by the similarity of the vibrational spectra attributed to the monomer in the gas, liquid and solid phases (see below). This is also consistent with the similarity of the structures of [CF₃$\overline{\text{CNSSN}}$]˙ **2d**[58] in the gas and solid phases, the only other carbon–sulfur–nitrogen radical for which experimental structures have been obtained in both gas and solid phases.

Both UB3PW91/6-31G* and UMPW1PW91/6-31+G* optimised geometries of radical **4d** were in satisfactory agreement with the structure determined by electron diffraction and X-ray crystallography (Table 7), taking into account the known elongation of bonds containing heavier elements at this level of theory[59] (SN bonds calculated to be too long by 0.03 to 0.04 Å). The calculated energy of rotating the SNS fragment out of the SCCS plane is very low (*e.g.* 3.9 kJ mol⁻¹ for 15° rotation, 18.5 kJ mol⁻¹ for 30°, 51.0 kJ mol⁻¹ for 45° (UB3PW91/6-31G*). A low energy has also been reported for the folding of **5** (5.0 kJ mol⁻¹ for 10°, 20.7 kJ mol⁻¹ for 20°)[19] and of a similar 1,3,2-dithiazolidine heterocycle in which the nitrogen bears a substituent hydrogen atom (0.0 kJ mol⁻¹ for 0°, 4.2 kJ mol⁻¹ for 36°).[60]

In the solid state **4d** monomers are associated into face-to-face dimers, shown in Fig. 7, by interaction of the two π* SNS based SOMOs (see Fig. 2 in Supplementary Material). However the monomers are not parallel. The dihedral angle between the planes containing each of the two rings is 26° resulting from the steric and electrostatic repulsion between the negatively charged CF₃ groups and cyclic carbon atoms (see Footnote **). In addition the sulfur–sulfur intermolecular distances are not

Table 7 Comparison of bond lengths (Å) and angles (°) for **3d**, radical **4d** and related species. E.s.d.s listed in parentheses

Parameter	3d calculated			4d					4h[c]	5[c]
	a	b	NBO bond order[b]	calc.[a]	calc.[b]	NBO bond order[b]	electron diffraction[c]	crystal structure[c]	crystal structure[18]	crystal structure[19]
Bond										
C=C	1.371	1.371	1.55	1.349	1.349	1.65	1.324 (7)	1.350 (4)	1.370 (6)	1.394 (3)
C–S	1.717	1.714	1.26	1.753	1.749	1.10	1.749 (3)	1.735 (3)	1.727 (5)	1.744 (2)
S–N	1.609	1.602	1.34	1.674	1.665	1.09	1.634 (2)	1.641 (3)	1.641 (4)	1.646 (2)
C–C	1.532	1.531	0.93	1.508	1.507	0.97	1.481 (3)	1.495 (5)	1.422 (8)	1.393 (3)
C–F	1.330	1.328	0.91	1.341	1.341	0.89	1.330 (2)	1.315 (8)		
Angle										
C=C–S	113.3	113.2		114.4	114.4		114.8 (3)	114.0 (2)	114.0 (4)	113.0 (2)
C–S–N	98.8	98.7		98.9	98.6		96.5 (6)	98.6 (2)	98.4 (2)	99.3 (1)
S–N–S	115.9	116.3		113.4	114.0		117.3 (5)	114.6 (2)	115.3 (3)	113.9 (1)
C–C–C	127.8	128.2		127.4	127.8		127.3 (3)	127.9 (3)	122.9 (5)	120.3 (2)
C–C–S	118.9	118.6		118.1	117.8		117.9 (3)	118.0 (3)	120.5 (4)	
Torsion angle										
S–C–C–S	0.26	0.40		0.03	0.11		0	0	0	0

[a] UB3PW91/6-31G*. [b] UMPW1PW91/6-31＋G*, averaged values; fully optimized geometry details have been deposited. [c] Averaged values.

equal [S(1)···S(8) 3.239 (36) Å; S(3)···S(6) 3.097 (50) Å] (ΣvdW radii = 3.6 Å) reflecting an angle between S(1)···S(3) and S(8)···S(6) of 3°. The dimers interact to give a tetramer, shown in Fig. 7, *via* six S···N contacts, two [S(3)···N(2)] at 3.190(3) Å lying in the same plane as the two centro-symmetrically related monomers they connect, and two sets of weaker contacts [S(6)···N(2) 3.302(3), S(3)···N(7) 3.199(3) Å], one set above and the other below the plane (ΣvdW radii (S···N) = 3.35 Å).[47] The non-centrosymmetric S···N contacts with the shorter of the two intra dimer sulfur contacts [S(3a)···S(6a), S(3b)···S(6b) 3.097(2) Å], and N(2a)··· N(7a) with N(7b)···N(2b), define a centrosymmetric rhombohedron (Fig. 7). The sulfur–nitrogen contacts are substantially ionic (calculated natural bond order (NBO) charges on the sulfur atoms of +0.71 and nitrogen −0.85), with the major portion of the bonding between the unpaired electrons of the monomer occurring in the S(3)N(2)–S(6)N(7) faces of the rhombohedron consistent with S(3)···S(6) being shorter than S(1)···S(8). Thus the covalent and ionic bonding of four monomer radicals in the observed tetramer largely occurs within the rhombohedral cage. The heats of fusion and sublimation are not significantly different from related diamagnetic molecules, therefore the magnitude of the sum of all the long inter-monomer interactions is very small.

The distances between the tetramer units are all significantly longer than those within the tetramer and are greater than the sum of the van der Waals radii of the atoms involved. A view of the crystal lattice of radical **4d** (as shown in Fig. 3 in the Supplementary Material) reveals that the tetramers are oriented to form layers with an internal sulfur–nitrogen rich zone sandwiched between layers of CF₃ groups. This would indicate that even though the interactions between the SNS areas of the tetramers are very long (and weak) they are sufficient to determine the larger structure of the lattice itself.

Dimers of radical **5**[20] are connected by planar sheets of long sulfur–sulfur contacts (four times 3.477(1), 3.781(1) Å per dimer). In contrast dimers of **4h**[23] are linked into a network polymer by ionic N–S interactions (see Fig 9A). There is no reason to assume that the strength of the two long completely covalent sulfur–sulfur bonds joining **4h** monomers of 3.145(2) Å [av.] are greater than the sum of largely ionic sulfur–nitrogen inter-dimer interactions. The solid state structure of [CF₃C̄NSSN]· consists of monomers connected by S···S [2.997(2) Å] and S···N bonds (3.197(5), 3.242(5) Å) formed by interaction of the two π* SOMOs.[58] However the dimers are
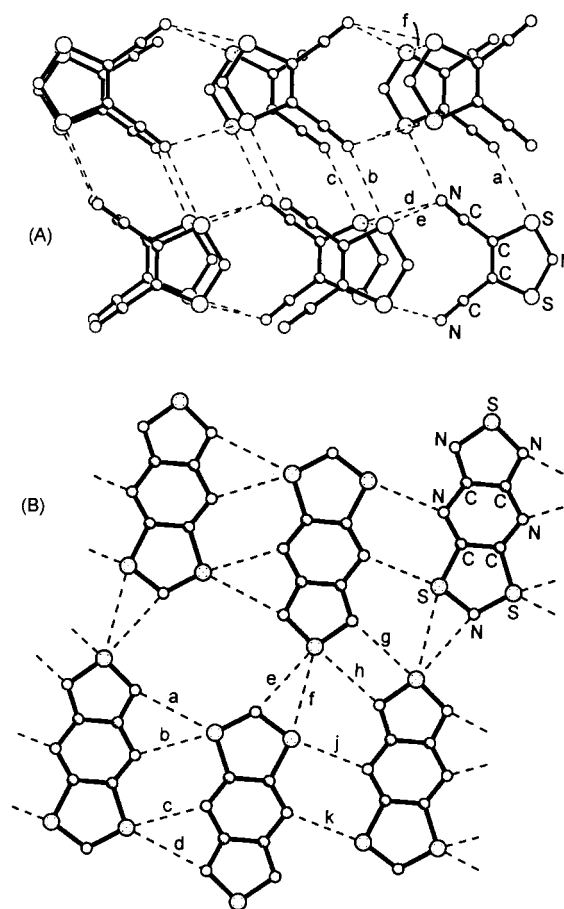

Fig. 9 Intermolecular contacts in radical **4h** (A) and **17** (B). Contacts for **4h**: a 3.275, b 2.126, c 3.275, d 3.222 and e 3.273 Å. Contacts for **17**: a 3.323, b 3.071, c 3.071, d 3.323, e 3.190, f 3.427, g 3.154, h 3.154, j 3.020 and k 3.020 Å.

joined by other long but significant S^{δ+}···N^{δ−} contacts into a three dimensional network. The importance of inter-monomer ionic S···N interactions is further illustrated by **17**,[21] which is a paramagnetic solid at room temperature. The overall structure of **17** is best described as consisting of monomers joined by largely ionic S···N interactions as shown in Fig. 9(B) into a sheet polymer. The sheets are equally separated and held apart,

we propose, largely by electrostatic repulsions, with monomers in each sheet arranged into slipped π stacks (Fig. 4 in reference 21c). The sulfur atoms are equally separated by 3.875(38) Å (less than twice Nyberg's isotropic sulfur vdW radius of 2.03 Å perpendicular to the π network). A phase transition at 150 K to a ground state antiferromagnetic material takes place in which electrons are paired by weak sulfur–sulfur π*–π* interactions [3.48(5) Å, SNS moiety, 3.401(5) Å, NSN fragment].

Gleiter and co-workers[58] showed that the two structurally different forms of the π*–π* [CF₃C̄NSSN]₂ dimer found in the solid state, as well as the alternative rotomers, were not significantly different in energy (<5 kJ mol⁻¹, MNDO calculations). The dimerisation energies in solution of simple monoradicals of this class are small (<40 kJ mol⁻¹) and solvent dependent[15] implying, but not proving, that the π*–π* bond energies of the pure radical were also small. The enthalpy of sublimation of radical **4d** is equal to the sum of the π*–π*, electrostatic and van der Waals intermolecular bond energy which is 49.0 kJ mol⁻¹ per monomer. The diamagnetic solid melts at 11.9 °C to give a paramagnetic liquid with $\Delta H_{\text{fusion}} = 11.5$ kJ mol⁻¹. If we assume that the electrostatic and van der Waals interactions are the same in the solid as in the liquid, then the enthalpy of fusion is equal to the strength of the π*–π* bond in the tetramer, i.e. 11.5 kJ mol⁻¹ per monomer, or 23.0 kJ mol⁻¹ per dimer, i.e. small and significantly less than the van der Waals and electrostatic interactions which are approximately 49.0 − 11.5 = 37.5 kJ mol⁻¹ per monomer. The dipole of **4d** is calculated to be 0.1 (UB3PW91/6-31G*) or 0.4 Debye (UMPW1PW91/6-31+G*), i.e. very small, and fluorine atoms are very non-polarisable, therefore van der Waals forces in **4d** are small. Therefore it is likely that the major contributions to the intermolecular interactions in solid and liquid **4d** are electrostatic, i.e. the interaction between $S^{0.64+}$ and $N^{0.77-}$ (UB3PW91/6-31G* Mulliken charges) on adjacent monomers in tetrameric (**4d**)₄ [see Fig. 7]. This is supported by dimerisation energy calculations which show the π*–π* dimer **19d** is not a stationary point. The triplet planar, centrosymmetric dimer **21d** given by two electrostatic $N^{0.61-} \cdots S^{0.53+}$ interactions at 3.109 Å (UB3PW91/6-31G* Mulliken charges, geometry and other details deposited) was stable by −7.8 kJ mol⁻¹.†† The corresponding calculated Mulliken charges (UB3PW91/6-31G*) on **4a** ($S^{0.43+}$, $N^{0.61-}$) are also appreciable, supporting the view that electrostatic interactions play a major role in determining the structures and physical properties of all the derivatives of **4**, and also in many of the related radicals derived from $[S_3N_2]^{+\cdot}$ (Scheme 1). We suggest that the planned synthesis of 7π C–N–S radicals of this class with specific structure and properties should take into account the importance of intramolecular electrostatic interactions.

The spectroscopic characterisation of radical 4d

The mass spectrum of radical **4d** is consistent with that of related compounds.[5] The solution ESR spectrum has been analysed elsewhere.[15] The ¹⁹F NMR spectra of neat **4d** shows one broad peak ($\gamma_{1/2} = 200$ Hz) at δ −59.7, but no peak is observed in dilute solution.

The UV-visible spectrum of radical **4d** in hexane is given in Fig. 3. The distinctive blue colour of the vapour of **4d** is presumably attributed to the weak red absorption at 738 nm ($\varepsilon = 110$ M⁻¹ cm⁻¹) in the gas phase and hexane solution, and the assigned transition based on high level theoretical calculations by Mattar, which will be published elsewhere.[56] The UV-vis spectrum of the related [HC̄NSSN]˙ has an absorption

at 617 nm that has been assigned by Oakley and co-workers to a π* ⟶ σ* transition.[61]

The vibrational spectra of radical 4d

The spectra of radical **4d** in all three states, and **3d**[AsF₆] salt, are shown in Figs. 1 and 2, with assignments based on the calculated spectra (geometries optimised to C_2 symmetry) given in Table 2. 33 vibrations are expected, all of which are both IR and Raman active. Of these, 27 are observed in the Raman spectrum of **4d**, 3 are calculated at lower frequency than the instrumental cut-off [Raman ≈ 90 cm⁻¹; IR ≈ 200 cm⁻¹].

Correlations between the observed and calculated frequencies are in good agreement for gaseous and liquid **4d**, and for solid **4d** in the high energy region (above 400 cm⁻¹), taking into account that the Raman spectrum of the solid is of better quality and that some peaks are split in the solid state. The major stretching vibrations remain similar for all phases of **4d** implying minimal changes in intramolecular bond distances on change of phase. Of particular note is the similarity of the C=C stretch for all three phases of **4d** (1580 cm⁻¹). This implies similar intramolecular bond distances in the solid and gas phases, although this cannot be concluded from the structural data because of the large deviations for the C=C distances, especially in the gas phase (see Table 7). The weak peak adjacent to the strong C=C stretching peak (1580 cm⁻¹) in the Raman spectra of **4d** is reasonably assigned to ¹³C isotope effects (ca. 4–6% observed relative peak height, 2.22% expected (¹³C natural abundance = 1.11%) relative intensity; 1.6% observed wavenumber difference, 2–4% expected by Hooke's law). The frequencies in the FT-Raman of solid **4d** below 250 cm⁻¹ are largely absent for the liquid and gaseous phase and, in part, can be attributable to intermolecular S · · · S and $S^{\delta+} \cdots N^{\delta-}$ vibrations between the monomers in the tetramer. Similar low energy absorptions in the Raman spectra of sulfur–nitrogen systems have been assigned to intermolecular long range S · · · S interactions in [HC̄NSSN]˙.[62] The calculated SN and CS distances in **4d** are longer than in **3d** (see below) consistent with the antibonding nature of the SOMO of **4d** and consistently **3d** SN and CS stretching frequencies are higher than those of **4d**. Similarly the C=C stretch is higher for **4d** than in **3d**, reflecting a shorter C=C distance and some bonding SOMO contribution.

The structure of liquid 4d as implied from its physical and spectroscopic properties

The structure of liquids is not readily determined, but we are able to deduce that of radical **4d** from its physical and spectroscopic properties. The Raman spectrum of the liquid in the bond stretching and bending regions is very similar indeed to that of the solid for which the crystal structure was determined. Thus the molecular structure is the same in both states, with the possible exception of some changes in the relative orientations of the two CF₃ groups to one another. The distance between molecules, however, is greater in the liquid as its molecular volume is ≈20% greater than the solid. The liquid is paramagnetic with weak antiferromagnetic intermolecular interactions reducing the magnetic moment from 1.53 to the observed 0 μ_B in the diamagnetic solid which consists of tetramers of weakly bound monomers. These facts imply that the liquid consists of monomers that are essentially separated by van der Waals distances. Consistently the heat of fusion is 11.5 kJ mol⁻¹, i.e. very low and similar to that of related diamagnetic molecules. This is an example of very small energy changes leading to dramatic changes in physical properties, in this case of volume, bulk magnetic properties and change in state. Other examples in this area include [p-NCC₆F₄C̄NSSN]˙ which is a spin canted antiferromagnet in one phase,[4] and **17** which becomes a paramagnetic solid with small structural changes on change of temperature,[21] and solid [N̄SNSC–

---

†† An overall diamagnetic tetramer may then be constructed by the addition of two radicals **4d** of appropriate spin to the centrosymmetric dimer.

Table 8 Observed IEs (eV) and calculated orbital energies (eV) for radical **4d**

Observed IE [a,b]	Orbital	ROMPW1PW(1/6-31+G* \ α	UMPW1PW91/6-31+G*		ROHF/6-31+G* \ α	UHF/6-31+G*	
			α	β		α	β
a: (7.46) 7.70	π (b$_1$)	2.95	5.97		2.87	8.94	
b: 10.85	π (a$_2$)[b]	9.29	9.73	9.06	11.69	12.82	11.12
c: 11.80	b	9.43	10.06	9.13	11.98	13.86	11.49
d: 12.50	b	9.80	10.10	9.67	13.71	13.94	13.41
e: 14.47	c	10.60	10.71	10.55	13.79	14.30	13.63
f: 15.55	c	12.32	12.36	12.22	16.01	16.33	15.69
g: 16.00	c	12.36	12.42	12.29	16.18	16.78	16.09
h: 17.24	c	12.42	12.59	12.33	16.63	18.00	16.52

[a] Letters correspond to labelling in Fig. 10; adiabatic first IE in parentheses. Calculated first IE [*E*(cation) − *E*(radical), UMPW1PW91/6-31+G*]: adiabatic = 7.67 eV, vertical = 7.92 eV. [b] See text. Bands b to d in Fig. 10 may comprise four π and σ orbitals (as suggested by the calculations), although only three distinct peaks are observed. [c] See text. Bands e to h in Fig. 10; maxima indicated, although total number of IEs and orbital assignments are not feasible.
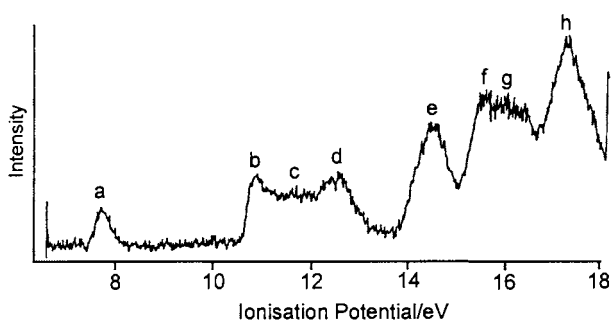
Fig. 10 Photoelectron spectrum of radical **4d**.

C̄SNSN]²⁻ which becomes a paramagnetic diradical on grinding.[63]

### Electronic structure and ultraviolet photoelectron spectroscopy (UPS) of radical 4d

The π and σ molecular orbitals (MOs) of radical **4d** (Fig. 2 in Supplementary Material) are consistent with lower level calculations for **4a** and **5**[20] and more extensive theoretical studies of aryl derivatives,[21] albeit with some delocalisation of ring MOs into the CF$_3$ substituents. The gas phase UPS of **4d** (Fig. 10), typical for such a radical, has a low-lying vertical IE at 7.70 eV (adiabatic, 7.46 eV), corresponding to ionisation from the singly occupied π MO of (in C$_{2v}$) b$_1$ symmetry. Following the first IE (Table 8) is a gap of some 3 eV to a cluster of 3 or 4 bands (labeled b–d) between 10.5 and 13.5 eV, which comprise ring π and σ MOs. Beyond 14 eV the remaining σ and π MOs contain increased CF$_3$ character, although the number of IEs and their assignment remain unknown. The calculated, *E*(cation) − *E*(radical), using UMPW1PW91/6-31+G* gives very satisfactory agreement for both adiabatic (a) (calc. 7.67 eV) and vertical (v) (calc. 7.92 eV) IEs, with the a − v difference (0.25 eV) matching that observed experimentally (0.24 eV), consistent with the relatively small geometry change between radical and cation (Table 7). Table 8 also shows the calculated orbital energies using the UMPW1PW91/6-31+G* and ROMPW1PW91/6-31+G* methods, together with single point ROHF and UHF (unrestricted Hartree–Fock) calculations at the UMPW1PW91/6-31+G* geometry. These are provided to assess the sequencing and spacing of the higher IEs, and to see if any Koopmans-like correspondence can be observed. The absolute values for these calculations are very poor, not surprisingly since Koopmans' theorem (IE = −ε_i) does not strictly hold for open shell systems, and for DFT there is the issue of the meaning of Kohn–Sham orbitals and eigenvalues. It has been suggested[64] that the ordering of Kohn–Sham orbitals is actually quite good when compared to conventional

ab initio methods and a simple scaling factor can be applied to bring the eigenvalues in accord with observed IEs. We have not undertaken this scaling exercise, but nonetheless the DFT results suggest, following the low lying IE, a cluster of 3 or 4 bands followed by a small gap before the remaining bands. Thus a Koopmans' like approach does seem to operate for such radicals[65] with DFT, although strictly it ignores the singlet–triplet splittings of the excited states of the cations. Previous experience with similar molecules[21b,65,66] suggests these exchange splittings are small.

Chemistry of radical 4d

Radical **4d** does not appear to react with O$_2$ at very low concentration in CCl$_3$F solution, but at higher concentration reaction occurred under various conditions, resulting in a foul smelling yellow oil containing a complex mixture [see Table 4, and Table 4 in the Supplementary Material]. The reaction of the radical **4d** with Cl$_2$ and Br$_2$ quantitatively produced the halide salts according to eqn. (5), and the reaction with arsenic

$$2\ \mathbf{4d} + X_2 \longrightarrow 2\ \mathbf{3d}[X] \qquad (5)$$
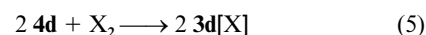
pentafluoride led to the formation of the salt **3d**[AsF$_6$] according to eqn. (6). The halides were fully characterised by

$$2\ \mathbf{4d} + 3\ AsF_5 \longrightarrow 2\ \mathbf{3d}[AsF_6] + AsF_3 \qquad (6)$$
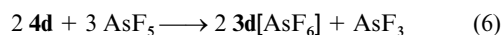
elemental analysis, mass spectra, infrared and NMR spectroscopy. They were readily purified by sublimation and could be reduced back to the radical with triphenylantimony. The halides **3d**[Cl] and **3d**[Br] could also be prepared by the metathetical reaction of **3d**[AsF$_6$] with CsCl and KBr, respectively, in liquid sulfur dioxide. The higher reactivity of the chloride salt with the solvent (giving SO$_2$Cl$_2$) required a more rapid isolation of the salt from the solvent and resulted in a lower yield by this route. Indeed, the attempted preparation of the fluoride by reaction of **3d**[AsF$_6$] with various fluorides in sulfur dioxide gave low yields of impure **4d** as the only isolable products.

Radical **4d** did not react with iodine, rather the neutral **4d** was generated by *in situ* formation of the iodide according to eqn. (7) in liquid sulfur dioxide solution, which then gave

$$2\ \mathbf{3d}[AsF_6] + 2\ CsI \longrightarrow \text{``}2\ \mathbf{3d}[I]\text{''} + 2\ Cs[AsF_6] \quad (7)$$
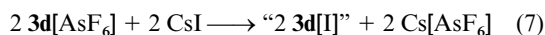
elemental iodine and **4d** according to eqn. (8). This is an

$$\text{``}2\ \mathbf{3d}[I]\text{''} \longrightarrow 2\ \mathbf{4d}\ (l) + I_2\ (s) \qquad (8)$$
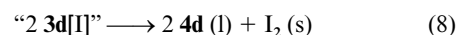
alternative preparative route to the radical **4d** which does not occur when the [AsF$_6$]⁻ salts of **3a** and **3b** are treated with

iodide. In these reactions, hydrolytically stable iodide salts are quantitatively recovered[25] according to eqn. (7). The relatively low first ionisation potential of **4d** (7.70 eV) is consistent with the facile oxidation of **4d** to the cation **3d** by elemental chlorine and bromine or AsF_5 but not iodine. Further studies of the thermodynamics of the system are in progress.[67]

Radical **4d** is rapidly hydrolysed by water but unreactive to the metals Cu and Hg and there was no observable reaction with the radical NO [Table 4, and Table 4 in the Supplementary Material].

Evidence for isolation of small quantities of radical 4c at −20 °C and its decomposition

The presence of a trifluoromethyl group as a substituent in derivative **4c** suggested that the radical may be isolable as a volatile species. ^{19}F NMR analysis of the *in situ* reduction of **3c**[AsF$_6$] by a mixture of tetramethylammonium chloride and triphenylantimony showed the quantitative reduction occurred almost instantaneously. However, **4c** decomposed to a myriad of diamagnetic non-volatile compounds at these concentrations within twenty minutes (^{1}H, ^{19}F NMR). The radical **4c** was isolated as a blue-black crystalline solid by fractional distillation of the volatiles immediately after reduction, which was very rapid. It was stable only if kept frozen (−196 °C) and was recovered as the chloride salt by reaction with chlorine. The stable chloride was shown spectroscopically (^{1}H, ^{19}F NMR) to be a mixture that contained a major component consistent with the cation **3c**. It is clear that the combination of rapid reduction and volatility, which allowed transfer to a trap at −196 °C, rather than stability allowed the isolation of this radical.
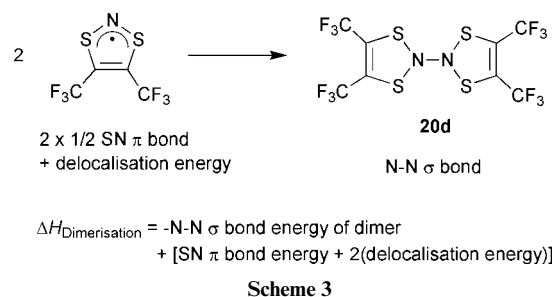
The decomposition of the radical **4c**, both as an isolated compound and in reaction mixtures, always produced a complex mixture of compounds (^{19}F NMR) in contrast to the rather simple products given on decomposition of **4d**. Sublimation of the non-volatile component of the reaction mixture allowed isolation of a diamagnetic, black crystalline solid in approximately 12% yield. Spectroscopic analysis by multinuclear NMR and mass spectroscopy indicated that the isolated compound was the thione **13**, identified by comparison with related compounds. The parent heterocycle 1,3,2-dithiazole-4-thione, $S\overline{CSNSC}H$, was generated by Oakley and co-workers from a complex mixture in low (> 5%) yield and characterised by single crystal X-ray crystallography.[44] More recently, a systematic study of the reaction of 1,3,2-dithiazolium chlorides with organic bases by Rees and co-workers[68] showed the thiones are produced in moderate yield. The fact that these reactions have retained the 1,3,2-dithiazolyl heterocyclic ring intact gives some indication of the chemical stability of this moiety.

The stability of $[R\overline{CSNSC}R]^{\cdot}$ radicals

The radicals **4a**–**4g** had been observed in dilute solution by ESR spectroscopy (Table 5), **4c**, **4e** and **4g** for the first time. The derivatives **4c** and **4g** were shown to have limited stability with observed half-lives of less than twenty minutes. We also attempted to prepare these radicals at higher (10^{-1} M) concentrations by reduction of the corresponding hexafluoroarsenate salt of **3**. The reactions either generated intractable, soluble tars (**4c**, **4e** and **4f**) or gave an insoluble black solid (**4a**), see Table 5. The solution of **4c** showed numerous peaks in the proton and/or fluorine NMR spectra, indicative of extensive decomposition (see below). **4d** and **4f** were the most stable in dilute solutions as measured by ESR spectroscopy (Table 5). However, when an attempt was made to isolate **4f** it decomposed at ≈ 0.1 M concentration after thirty-six hours and on attempted isolation after rapid reduction. This pattern of stability is very similar to that observed for **4i** which we reported as a stable radical in solution with concentrations less than 0.5 M.[7]

The stability of radical **4d** is similar to that of the corresponding bis(perfluoromethyl)aminyl oxide radical $(CF_3)_2NO$.[69] The dimethylaminyloxide is not isolable, however $[(CH_3)_3-C_2]NO$ is,[45] whereas the related **4f**, sterically protected by the $(CH_3)_3Si$ groups, is not. Thus it does not seem that moderately bulky substituents will lead to stable derivatives of **4** as is the case for the aminyl oxides. It is significant that **4c**‡‡ was isolated at low temperature by rapidly removing it from the reduction mixture. This suggests that derivatives of **4** may be isolated if they can be rapidly removed from the reaction mixture to either low pressure and/or low temperature conditions. However, it rapidly decomposed to numerous products when warmed to room temperature, even when removed from the reaction mixture and dissolved in relatively dilute solution. Similarly, Wolmershäuser and Kraft have shown that the dicyano derivative **4h** is a stable species that can be isolated[23] while **4g** rapidly decomposes even in dilute solution, and **4a**, **4b**, **4e**, **4f** all decomposed. This suggests all derivatives of **4** containing hydrogen are liable to have low stability with respect to decomposition. The concentration dependence of the stabilities of **4f** and **4i**[7] and the quantitative nature of the decomposition of **4d** implies that the decomposition is bi- or multi-molecular.
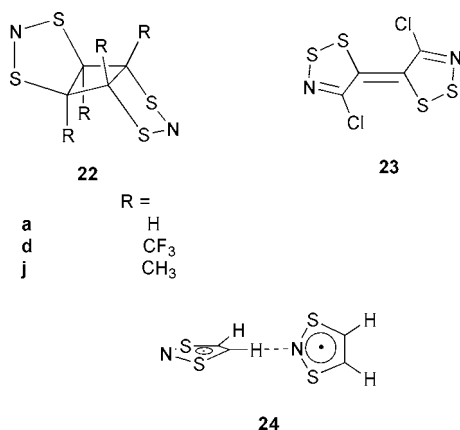
Radical **5**[19,20] and various other related benzenoid derivatives, as well as **4d** and **4h**, are isolatable as pure materials under ambient conditions. This suggests that the stability of these radicals may be associated with a lowering of the bonding π orbital energies by delocalisation into the aryl ring for **5**[19] and on to the substituent for **4d** (*e.g.* MOs SOMO-9, SOMO-14 in Fig. 2 of Supplementary Material) and implied by the structure of **4h**, as well as lowering of energy by the inductive effect of the electronegative substituents as expected for **4d** and **4h**. The dimerisation energies of **4a** and **4d** to monomers linked into dimers through N–N, S–S or S–N σ bonds were expected to be more favourable for **4a** than **4d** due to the stronger, more delocalised π bonds in **4d** that would be broken to form the dimer (shown in Scheme 3 for **4d**, with an N–N bonding dimer).

$$\Delta H_{Dimerisation} = \text{-N-N σ bond energy of dimer} \\ + [\text{SN π bond energy} + 2(\text{delocalisation energy})]$$

Scheme 3

In fact, the enthalpies (UB3PW91/6-31G*) of dimerisation of the N–N σ bonded dimer **20** of **4a**, **4j**, and **4d** are all about zero, and the free energies are all unfavourable. Other σ bonded dimers are of higher energy than that of the N–N dimer **20**. However, a triplet σ dimer **22** bonded through both carbons is favoured for **4a** ($\Delta H_{dimerisation} = -47.4$ kJ mol^{-1}, $\Delta G_{dimerisation} = 17.0$ kJ mol^{-1}), thermally accessible for **4j** ($\Delta H_{dimerisation} = 6.1$ kJ mol^{-1}, $\Delta G_{dimerisation} = 90.1$ kJ mol^{-1}), but unfavourable for **4d** ($\Delta H_{dimerisation} = 44.6$ kJ mol^{-1}, $\Delta G_{dimerisation} = 124.5$ kJ mol^{-1}) (C–C bond distances: for **22a**, 1.550 and 1.553; **22j**, 1.572 and 1.581; **22d**, 1.573 and 1.592 Å). This implies that the decompostions of **4a** and **4j** may proceed through the formation of the dimer **22**. Similar reactions have been found for the related $Cl\overline{CNSSC}Cl$ radical, which rapidly dimerised *via* a C–C bond and led to **23**.[48] Attempts to investigate the face-to-face dimer **19a** optimised to a triplet state hydrogen bonded dimer **24** through a H···C bond of 2.334 Å,

---

‡‡ We note, however, that there were no significant differences in the decomposition products when radical **4c** was isolated and when it remained in the presence of the reducing agents in the reaction mixture.

and a dihedral angle between the rings of 88.7°, with the enthalpy and free energy of dimerisation of −12.4 and 26.1 kJ mol⁻¹, respectively. This provides for additional reaction pathways for **4a** and C–H hydrogen containing derivatives of **4**, consistent with the greater reactivity of **4a**. The concentration dependence of the stability of **4a, 4b, 4c, 4e, 4f** and **4i**[7] and the quantitative nature of the decomposition of **4d** indicates that the decomposition is multimolecular, which is supported by our calculations.

22   **23**

R =
a   H
d   CF₃
j   CH₃

24

Acknowledgements

References

1 (a) A. J. Banister and J. M. Rawson, in *The Chemistry of Inorganic Ring Systems*, ed. R. Steudel, Elsevier, Amsterdam, 1992; (b) A. J. Banister and J. M. Rawson, *Adv. Heterocycl. Chem.*, 1995, **62**, 137; (c) R. T. Oakley, *Prog. Inorg. Chem.*, 1988, **36**, 299; (d) A. W. Cordes, R. C. Haddon and R. T. Oakley, in *The Chemistry of Inorganic Ring Systems*, ed. R. Steudel, Elsevier, Amsterdam, 1992; (e) R. T. Oakley, *Can. J. Chem.*, 1993, **71**, 1775; (f) J. M. Rawson, *New J. Chem.*, 1999, **23**, 565.

2 *Comprehensive Heterocyclic Chemistry*, eds. A. R. Katritsky and C. W. Rees, Pergamon Press, Oxford, 1984.

3 T. M. Barclay, A. W. Cordes, R. C. Haddon, M. E. Itkis, R. T. Oakley, R. W. Reed and H. Zhang, *J. Am. Chem. Soc.*, 1999, **121**, 969.

4 A. J. Banister, N. Bricklebank, I. Lavender, J. M. Rawson, C. I . Gregory, B. K. Tanner, W. Clegg, M. R. J. Elsegood and F. Palacio, *Angew. Chem.*, *Int. Ed. Engl.*, 1996, **35**, 2533.

5 (a) G. K. MacLean, J. Passmore, M. N. S. Rao, M. J. Schriver, P. S. White, D. Bethell, R. S. Pilkington and L. H. Sutcliffe, *J. Chem. Soc.*, *Dalton Trans.*, 1985, 1405; (b) S. Parsons, J. Passmore, M. J. Schriver and X. Sun, *Inorg. Chem.*, 1991, **30**, 3342.

6 M. Sannigrahi and F. Grein, *J. Mol. Struct. (Theochem)*, 1999, **465**, 25.

7 S. Parsons and J. Passmore, *Acc. Chem. Res.*, 1994, **27**, 101.

8 A. J. Banister, H. G. Clarke, I. Rayment and H. M. M. Shearer, *Inorg. Nucl. Chem. Lett.*, 1974, **10**, 647.

9 T. S. Cameron, R. C. Haddon, S. M. Mattar, S. Parsons, J. Passmore and A. P. Ramirez, *J. Chem. Soc.*, *Dalton Trans.*, 1992, 1563.

10 T. S. Cameron, R. C. Haddon, S. M. Mattar, S. Parsons, J. Passmore and A. P. Ramirez, *Inorg. Chem.*, 1992, **31**, 2274.

11 J. Passmore, X. Sun and S. Parsons, *Can. J. Chem.*, 1992, **70**, 2972.

12 N. Burford, J. Passmore and M. J. Schriver, *J. Chem. Soc.*, *Chem. Commun.*, 1986, 140.

13 A. Vegas, A. Pérez-Salazar, A. J. Banister and R. G. Hey, *J. Chem. Soc.*, *Dalton Trans.*, 1980, 1812.

14 G. K. MacLean, J. Passmore, M. J. Schriver, P. S. White, D. Bethell, R. S. Pilkington and L. H. Sutcliffe, *J. Chem. Soc.*, *Chem. Commun.*, 1983, 807.

15 (a) S. R. Harrison, R. S. Pilkington and L. H. Sutcliffe, *J. Chem. Soc.*, *Faraday Trans. 1*, 1984, 669; (b) S. A. Fairhurst, R. S. Pilkington and L. H. Sutcliffe, *J. Chem. Soc.*, *Faraday Trans. 1*, 1983, 925; (c) S. A. Fairhurst, R. S. Pilkington and L. H. Sutcliffe, *J. Chem. Soc.*, *Faraday Trans. 1*, 1983, 439; (d) K. F. Preston and L. H. Sutcliffe, *Magn. Reson. Chem.*, 1990, **28**, 189; (e) Y.-L. Chung, S. A. Fairhurst, D. G. Gilles, K. F. Preston and L. H. Sutcliffe, *Magn. Reson. Chem.*, 1992, **30**, 666.

16 Y. Miura, N. Makita and M. Kinoshita, *Bull. Chem. Soc. Jpn.*, 1977, **50**, 482; Y. Miura, N. Makita and M. Kinoshita, *Tetrahedron Lett.*, 1975, 127; Y. Miura and M. Kinoshita, *Bull. Chem. Soc. Jpn.*, 1980, **53**, 2395.

17 K. Schlosser and S. Steenken, *J. Am. Chem. Soc.*, 1983, **105**, 1504.

18 J. S. Thrasher and J. B. Neilsen, *J. Am. Chem. Soc.*, 1986, **108**, 1108.

19 G. Wolmershäuser, M. Schnauber and T. Wilhelm, *J. Chem. Soc.*, *Chem. Commun.*, 1984, 573.

20 E. G. Awere, N. Burford, R. C. Haddon, S. Parsons, J. Passmore, J. V. Waszczak and P. S. White, *Inorg. Chem.*, 1990, **29**, 4821.

21 (a) T. M. Barclay, A. W. Cordes, N. A. George, R. C. Haddon, R. T. Oakley, T. T. M. Palstra, G. W. Patenaude, R. W. Reed, J. F. Richardson and H. Zhang, *Chem. Commun.*, 1997, 873; (b) T. M. Barclay, A. W. Cordes, R. H. de Laat, J. D. Goddard, R. C. Haddon, D. Y. Jeter, R. C. Mawhinney, R. T. Oakley, T. T. M. Palstra, G. W. Patenaude, R. W. Reed and N. P. C. Westwood, *J. Am. Chem. Soc.*, 1997, **119**, 2633; (c) T. M. Barclay, A. W. Cordes, N. A. George, R. C. Haddon, M. E. Itkis, M. S. Mashuta, R. T. Oakley, G. W. Patenaude, R. W. Reed, J. F. Richardson and H. Zhang, *J. Am. Chem. Soc.*, 1998, **120**, 352; (d) W. Futijta and K. Auaga, *Science*, 1999, **286**, 261.

22 (a) E. G. Awere, N. Burford, C. Mailer, J. Passmore, M. J. Schriver, P. S. White, A. J. Banister, H. Oberhammer and L. H. Sutcliffe, *J. Chem. Soc.*, *Chem. Commun.*, 1987, 66; (b) W. V. F. Brooks, N. Burford, J. Passmore, M. J. Schriver and L. H. Sutcliffe, *J. Chem. Soc.*, *Chem. Commun.*, 1987, 69.

23 G. Wolmershäuser and G. Kraft, *Chem. Ber.*, 1990, **123**, 881.

24 S. Brownridge, T. S. Cameron, J. Passmore, G. Schatte and T. C. Way, *J. Chem. Soc.*, *Dalton Trans.*, 1996, 2553; M.P. Murchie, J. Passmore and R. Kapoor, *Inorg. Synth.*, 1997, **31**, 102.

25 M. J. Schriver, Ph.D. Thesis, University of New Brunswick, 1988.

26 M. Alace and N. P. C. Westwood, *J. Phys. Chem.*, 1994, **98**, 3818.

27 HyperChem 3.0 for Windows, Autodesk, Hypercube, Inc., Gainsville, FL, 1993.

28 W. L. Jolly, *The Synthesis and Characterisation of Inorganic Compounds*, Prentice Hall, New York, 1970.

29 W. Bludssus and R. Mews, *J. Chem. Soc.*, *Chem. Commun.*, 1979, 35.

30 C. G. Krespan, B. C. McKusick and T. L. Cairns, *J. Am. Chem. Soc.*, 1960, **82**, 1515; C. G. Krespan, *J. Am. Chem. Soc.*, 1961, **83**, 3434.

31 H. Oberhammer, in *Molecular Structure by Diffraction Methods*, The Chemical Society, London, 1976.

32 H. Oberhammer, W. Gombler and H. Willner, *J. Mol. Struct.*, 1980, **70**, 273.

33 H. Bürger, G. Pawelke and H. Oberhammer, *J. Mol. Struct.*, 1982, **84**, 49.

34 J. Haase, *Z. Naturforsch.*, *Teil A*, 1970, **25**, 936.

35 J. Cosier and A. M. Glazer, *J. Appl. Crystallogr.*, 1986, **19**, 105.

36 A. J. M. Duisenberg, *J. Appl. Crystallogr.*, 1992, **25**, 92.

37 P. T. Beurskens, G. Beurskens, W. P. Bosman, R. de Gelder, S. Garcia-Granda, R. O. Gould, R. Isreal and J. M. M. Smits, The DIRDIF-96 program system, Crystallographic Laboratory, University of Nijmegen, 1995.

38 G. M. Sheldrick, SHELXTL version 5, Siemens Analytical Instrumentation Inc., Madison, WI, 1995.

39 GAUSSIAN 94, Revision E.3, M. J. Frisch, G. W. Trucks, H. B. Schlegel, P. M. W. Gill, B. G. Johnson, M. A. Robb, J. R. Cheeseman, T. Keith, G. A. Petersson, J. A. Montgomery, K. Raghavachari, M. A. Al-Laham, V. G. Zakrzewski, J. V. Ortiz, J. B. Foresman, J. Cioslowski, B. B. Stefanov, A. Nanayakkara, M. Challacombe, C. Y. Peng, P. Y. Ayala, W. Chen, M. W. Wong, J. L. Andres, E. S. Replogle, R. Gomperts, R. L. Martin, D. J. Fox, J. S. Binkley, D. J. Defrees, J. Baker, J. P. Stewart, M. Head-Gordon, C. Gonzalez and J. A. Pople, Gaussian, Inc., Pittsburgh, PA, 1995.

40 GAUSSIAN 98 (Revision A.3), M. J. Frisch, G. W. Trucks, H. B. Schlegel, G. E. Scuseria, M. A. Robb, J. R. Cheeseman, V. G. Zakrzewski, J. A. Montgomery, R. E. Stratmann, J. C. Burant, S. Dapprich, J. M. Millam, A. D. Daniels, K. N. Kudin, M. C. Strain, O. Farkas, J. Tomasi, V. Barone, M. Cossi, R. Cammi, B. Mennucci, C. Pomelli, C. Adamo, S. Clifford, J. Ochterski, G. A. Petersson, P. Y. Ayala, Q. Cui, K. Morokuma, D. K. Malick, A. D. Rabuck, K. Raghavachari, J. B. Foresman, J. Cioslowski, J. V. Ortiz, B. B. Stefanov, G. Liu, A. Liashenko, P. Piskorz, I. Komaromi, R. Gomperts, R. L. Martin, D. J. Fox, T. Keith, M. A. Al-Laham, C. Y. Peng, A. Nanayakkara, C. Gonzalez, M. Challacombe, P. M. W. Gill, B. G. Johnson, W. Chen, M. W. Wong, J. L. Andres, M. Head-Gordon, E. S. Replogle and J. A. Pople, Gaussian, Inc., Pittsburgh, PA, 1998.
41 J. B. Foresman and A. Frisch, *Exploring Chemistry with Electronic Structure Methods*, 2nd edn., Gaussian Inc., Pittsburgh, PA, 1995.
42 F. de Proft and P. Geerlings, *J. Chem. Phys.*, 1997, **106**, 3270.
43 S. Joanteguy, G. Pfister-Guillouzo and H. Chermette, *J. Phys. Chem.*, 1999, **103**, 3505.
44 R. T. Oakley, University of Guelph, personal communication; R. T. Oakley, H. Koenig and A. W. Cordes, *Acta Crystallogr.*, *Sect. C*, 1987, **43**, 2468.
45 Aldrich Chemical Company Inc., *Catalogue Handbook of Fine Chemicals 1996–1997*, Milwaukee, 1996.
46 E. Awere, N. Burford and J. Passmore, unpublished work.
47 J. E. Huheey, E. A. Kieter and R. L. Kieter, *Inorganic Chemistry*, 4th edn., Harper Collins Publishers, New York, 1993.
48 T. M. Barclay, L. Beer, A. W. Cordes, R. C. Haddon, M. I. Itkis, R. T. Oakley, K. E. Preuss and R. W. Reed, *J. Am. Chem. Soc.*, 1999, **121**, 6657.
49 E. A. Moelwyn-Hughes, *Physical Chemistry*, 2nd edn., MacMillan, New York, 1961.
50 S. C. Nyburg and C. H. Faerman, *Acta Crystallogr.*, *Sect. B*, 1985, **41**, 274.
51 Z. V. Hauptman and A. J. Banister, personal communication.
52 M. I. Hansford, Ph.D. Thesis, Durham University, 1989.
53 S. A. Fairhurst, K. M. Johnson, L. H. Sutcliffe, K. F. Preston, A. J. Banister, Z. V. Hauptman and J. Passmore, *J. Chem. Soc.*, *Dalton Trans.*, 1986, 1465; J. Passmore and X. Sun, *Inorg. Chem.*, 1996, **35**, 1313.
54 C. K. Johnson, ORTEP II, Report ORNL-5138, Oak Ridge National Laboratory, Oak Ridge, TN, 1976.
55 U. Englert, J. Passmore, M. J. Schriver and R. Strähle, unpublished work.
56 S. Mattar and A. D. Stephens, *J. Phys. Chem.*, 2000, **104**, 3718.
57 A. Domenicano and I. Hargittai (Editors), *Accurate Molecular Structures*, Oxford University Press, Oxford, 1992.
58 H.-U. Höfs, J. W. Bats, R. Gleiter, G. Hartmann, R. Mews, M. Eckert-Maksic, H. Oberhammer and G. M. Sheldrick, *Chem. Ber.*, 1985, **118**, 3781.
59 R. Haist, R. M. S. Alvartez, E. H. Cutin, C. O. Della Vedora and H. Oberhammer, *J. Mol. Struct.*, 1999, **484**, 249.
60 M. J. S. Dewar, H. W. Kollmar and S. H. Suck, *Theor. Chim. Acta*, 1975, **36**, 237; R. Boese, H. Oberhammer, P. Pulay and A. Waterfeld, *J. Phys. Chem.*, 1993, **97**, 9625.
61 J. Campbell, D. Klapstein, P. F. Bernath, W. M. Davis, R. T. Oakley and J. D. Goddard, *Inorg. Chem.*, 1996, **35**, 4264.
62 C. D. Bryan, A. W. Cordes, R. C. Haddon, R. G. Hicks, D. K. Kennepohl, C. D. MacKinnon, R. T. Oakley, T. T. M. Palstra, A. S. Perel, S. R. Scott, L. F. Schneemeyer and J. V. Waszczak, *J. Am. Chem. Soc.*, 1994, **116**, 1205; N. Burford, T. Chivers, P. W. Codding and R. T. Oakley, *Inorg. Chem.*, 1982, **21**, 982.
63 W. V. F. Brooks, S. Brownridge, S. Parsons and J. Passmore, *Phosphorus Sulfur Silicon Relat. Elem.*, 1994, **93–94**, 443; G. Antorrena, S. Brownridge, T. S. Cameron, F. Palacio, S. Parsons, J. Passmore and L. K. Thompson, *Inorg. Chem.*, to be published.
64 R. Stowasser and R. Hoffmann, *J. Am. Chem. Soc.*, 1999, **121**, 3414.
65 R. T. Boeré, R. T. Oakley, R. W. Reed and N. P. C. Westwood, *J. Am. Chem. Soc.*, 1989, **111**, 1180.
66 A. W. Cordes, C. D. Bryan, W. M. Davis, R. H. de Laat, S. H. Glarum, J. D. Goddard, R. C. Haddon, R. G. Hicks, D. K. Kennepohl, R. T. Oakley, S. R. Scott and N. P. C. Westwood, *J. Am. Chem. Soc.*, 1993, **115**, 7232.
67 D. Jenkins, J. Passmore and M. J. Schriver, to be published.
68 P. J. Dunn and C. W. Rees, *J. Chem. Soc.*, *Perkin Trans. 1*, 1989, 2489; M. A. Gray and C. W. Rees, *J. Chem. Soc.*, *Perkin Trans. 1*, 1993, 3077; J. L. Morris and C. W. Rees, *J. Chem. Soc.*, *Perkin Trans. 1*, 1987, 217.
69 (*a*) A. K. Hoffmann and A. T. Henderson, *J. Am. Chem. Soc.*, 1961, **83**, 4671; (*b*) W. D. Blackley and R. R. Reinhard, *J. Am. Chem. Soc.*, 1965, **87**, 802.